AN ABSTRACT OF THE THESIS OF

MICHAEL DONAVON BRADY for the DOCTOR OF PHILOSOPHY
(Name) (Degree)

in CHEMICAL ENGINEERING presented on Dec. 13, 1968
(Major) (Date)

Title: A STUDY OF THERMAL EFFECTS INVOLVED IN THE PERFORMANCE OF A WETTED-WALL COLUMN

Abstract approved [redacted]
Dr. C. E. Wicks

The distillation of a two component system in a wetted-wall column operating at total reflux was investigated without an external heat source and with an external heat source. The number of transfer units based on the overall vapor phase concentration driving force was calculated using the recommended equation for equimolar mass transfer. The results for the case with no external heat source was compared with analogy equations based on data from gas absorption investigations. The difference between the gas absorption predictions and the experimental results were shown to be due to the thermal effects which exist in distillation operations but do not exist in gas absorption operations.

An equation was developed which showed that the original definition for the number of transfer units needed to be modified to include the thermal effects and non-equimolar counterdiffusion. This

modified equation was used to analyze data that had been influenced by external heat sources and was found to agree with the experimental data. The individual terms in the internal thermal effects were estimated to show their relative effect on the separation obtained.

A 2.54-cm O.D. glass wetted-wall column, 122-cm in length, was used. The column was surrounded by a 7.62-cm O.D. glass column through which heating and cooling solutions were circulated. The binary mixture benzene-n-butanol was used in the investigation because the system possessed a fairly high relative volatility, 4.5, and because good vapor-liquid equilibrium data were available. The temperature at eight points in the system was recorded using thermocouples.

The results of this study are:

1. The form of the equation for the number of transfer units with adiabatic thermal effects, $\phi(y_A, y_{Ai})$, and non-adiabatic thermal effects, $\phi'(y_A, y_{Ai}, T_b)$ is given in the following equation.

$$N'_{OG} = \int_{y_{AO}}^{y_{AT}} \frac{dy_A}{(y_A^* - y_A) + \phi(y_A, y_{Ai}) + \phi'(y_A, y_{Ai}, T_b)}$$

   This was based on mass and energy balances.

2. The modified form N'_{OG} has been shown to describe the performance of a wetted-wall column when $\phi'(y_A, y_{Ai}, T_b) \gg \phi(y_A, y_{Ai})$.

A Study of Thermal Effects Involved in the Performance of a Wetted-Wall Column

by

Michael Donavon Brady

A THESIS

submitted to

Oregon State University

in partial fulfillment of
the requirements for the
degree of

Doctor of Philosophy

June 1969

APPROVED:

[redacted]

Professor of Chemical Engineering

in charge of major

[redacted]

Head of Department of Chemical Engineering

[redacted]

Dean of Graduate School

Date thesis is presented Dec. 13, 1968

Typed by Clover Redfern for Michael Donavon Brady

ACKNOWLEDGMENTS

I wish to extend by grateful appreciation to the following:

To Dr. C. E. Wicks for his professional assistance and encouragement throughout the duration of this investigation.

To the National Science Foundation and to the Oregon State University Engineering Experiment Station for their financial support during this study.

To William B. Johnson for his contributions to the construction of experimental equipment.

To Richard Maier for his excellent glass blowing contributions.

To my wife, Janice Kay, for encouragement throughout the duration of my graduate career.

To My Loving Wife

TABLE OF CONTENTS

LIST OF FIGURES

LIST OF TABLES

A STUDY OF THERMAL EFFECTS INVOLVED IN THE PERFORMANCE OF A WETTED-WALL COLUMN

INTRODUCTION

Fractional distillation is an important unit operation used to separate the components of a liquid mixture. If the components of the mixture possess different vapor pressure at a given temperature, a separation results in which a vapor richer in the more volatile component and a liquid richer in the less volatile component is produced.

In the design of a distillation system, the engineer must be able to predict the amount of separation or mass transfer which will take place. Previous distillation design techniques for continuous contact operations have considered the concentration difference between the vapor and the liquid phases as the only driving force of any importance. Several simplifying assumptions about the energy exchange between the phases must be made for this to be true. Frequently, the major assumption of negligible thermal effects is made without any verification.

Kirschbaum (19) was the first to consider the importance of thermal effects. The theory suggested by Kirschbaum was ignored for many years until interest was again revived in a discussion at a recent symposium on distillation (8).

The primary thermal effect, called thermal distillation, involves

the heat transfer from the vapor phase to the liquid phase. The effect is thought to exhibit itself in two different manners. The first is the obvious effect that energy is transferred from the hotter vapor to the cooler liquid and thus supplies more energy for vaporization. The net effect being, to facilitate a greater separation for the same amount of contact area. During the distillation symposium it was suggested that the magnitude of the energy transferred could be estimated by using the Chilton-Coburn analogy between heat and mass transfer (5). The system, ethanol-water, was cited as an example. With a maximum temperature difference of 12° C between the vapor and liquid, the amount of heat transferred due to the temperature difference between the phases was about 5. 3 percent of the heat transferred by the latent heat of vaporization of the less volatile component.

The second thermal effect develops as a result of the concentration and temperature gradients within the liquid phase. Since the thermal diffusivity in the vapor phase is similar in value to the mass diffusivity in the vapor, the thermal gradient within the phase is analogous to the concentration gradient. Accordingly, energy is transferred to the liquid interface at essentially the same rate as the mass is transferred. This similarity in rates of transfer is not true in the liquid phase where the thermal diffusivity is much larger than the mass diffusivity. Concentration and temperature profiles, similar to those

shown in Figure 1, are developed during steady-state operation. The temperature gradient extends deeper into the liquid phase than does the concentration gradient.

Because of the variation in temperature and concentration gradients, energy is transferred into the liquid faster than the mass is transferred. Accordingly, the temperature of the liquid at a level below the surface can approach its bubble-point and flash distillation results. The flashing effect produces vapor bubbles which provide a mixing effect within the liquid. The resistance to mass transfer within the liquid is reduced by the mixing effect. Since the necessary concentration and thermal gradients are more likely to be established in systems of high relative volatility (8), the flashing and the mixing effect will be more important in systems of high relative volatility than in systems where the components have similar vapor pressures.

The present author wishes to investigate the thermal distillation phenomenon, specifically to develop the model which describes the simultaneous heat and mass transfer operations and then to verify how the thermal effects can influence the performance of a distillation operation.

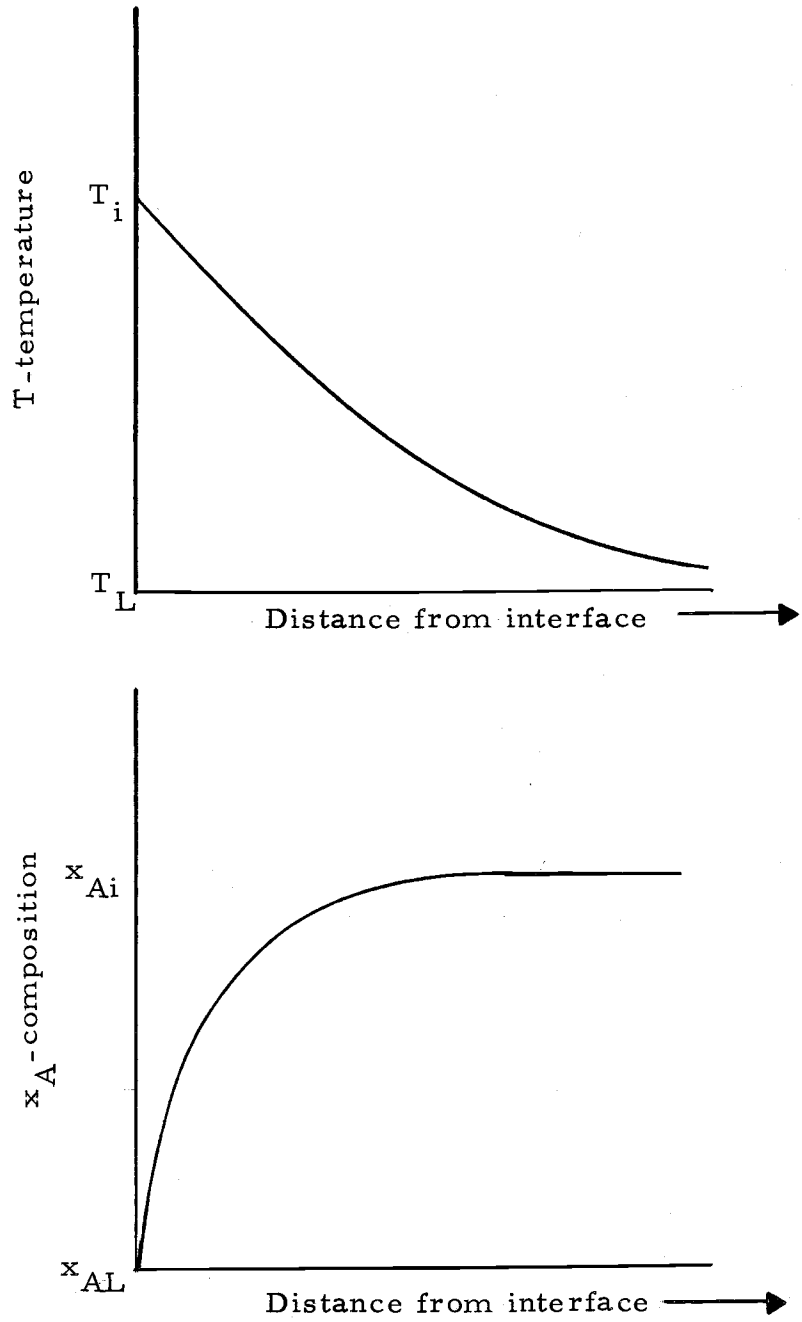

Figure 1. Temperature and concentration profiles in the liquid.

DISCUSSION OF PREVIOUS WORK

The most common method of predicting the performance of a continuous contact operation is the use of transfer units. By definition, the height of a column required for a specified separation is the product of the number of transfer units, N_{OG}, and the height of a transfer unit, H_{OG}. The origin and use of these equations are discussed in the original presentations (4, 6). The definition of the number of transfer units with equimolar counterdiffusion is given in Equation (1).

$$N_{OG} = \int_{y_{AO}}^{y_{AT}} \frac{dy_A}{(y_A^* - y_A)} \tag{1}$$

The definition of the height of a transfer unit is given in Equation (2).

$$H_{OG} = \frac{G}{K_G a} \tag{2}$$

The symbols used in the equations and discussions are defined in the nomenclature section.

In distillation the value of N_{OG} shows a large variation with the gas phase composition over the more-volatile component mole fraction range of zero to one (11, 17, 22, 27, 30). In these investigations, the equation for N_{OG}, Equation (1), was always used even

though equimolar counterdiffusion did not exist.

Zuiderweg and Harmens (36) and Danckwerts, Sawistowski and Smith (8) showed the number of transfer units for a column varies as the surface tension of the liquid changes. This would appear only where the change in surface tension of the liquid with an increase in mole fraction of the more-volatile component is greater than zero. The liquid film in this case will break up into small streams and thus cause a decrease in the surface area of the liquid. Since the amount of mass transfer possible is directly proportional to the liquid surface area, there will be a corresponding decrease in the possible separation.

Sawistowski and Smith (30) attempted to show that the variation of the column efficiency, or number of transfer units N_{OG}, with the change in the average composition of the vapor inlet and outlet, $\frac{1}{2}(y_{AO}+y_{AT})$, could not be completely accounted for by the variation in fluid properties. A packed column was used to make the investigations. The binary mixtures distilled were carbon tetrachloride-toluene, cyclohexane-toluene, and n-heptane-toluene. The experimental results were used to calculate the number of transfer units, N_{OG}, using Equation (1). The resulting values of N_{OG} were graphed as a function of $\frac{1}{2}(y_{AO}+y_{AT})$, the arithmetic average of the inlet and outlet compositions, and were found to vary from 50 to 75 percent for each of the systems. Data were taken over most of the

composition range for $\frac{1}{2}(y_{AO}+y_{AT})$. The experimental data were then used to calculate N_{OG} by predicting the mass transfer coefficients on each side of the interface. The equation used to predict the liquid side mass transfer coefficient, k_L, was that suggested by Chari and Storrow (3). The vapor side mass transfer coefficient, k_G, was that suggested by Pratt (26). The variation of k_L and k_G and the variation in the slope of the equilibrium line were then used to predict the variation of N_{OG} with composition. Analyzing experimental data for the three systems, the variation could not be completely explained by the variation in the physical properties.

The performance of an adiabatic wetted-wall column was studied by Quershi and Smith (27). The number of transfer units, N_{OG}, were measured as a function of $\frac{1}{2}(y_{AO}+y_{AT})$. Results for the binary mixtures acetone-benzene, chloroform-benzene, acetone-chloroform, heptane-methyl cyclohexane, heptane-toluene, and methyl cyclohexane-toluene were given. The graph of H_{OG} versus $\frac{1}{2}(y_{AO}+y_{AT})$ had a minimum at some intermediate composition with H_{OG} becoming very large when the average mole fraction, $\frac{1}{2}(y_{AO}+y_{AT})$, approached zero and one. These were similar to the plots of Sawistowski and Smith (30) for a packed column. Quershi and Smith (27) multiplied H_{OG} by $y_A(1-y_A)$ and plotted this versus $\frac{1}{2}(y_{AO}+y_{AT})$. The resulting product had less variation with

composition than did H_{OG}. It was found that $y_A(1-y_A)^{1.35}$ gave a better result for heptane-toluene. In doing so, the authors were trying to find a suitable equation for predicting H_{OG} which was independent of composition. The product $H_{OG}y_A(1-y_A)^n$ did approach a horizontal line, but the value of n was different for each mixture. The authors felt this simple modification was adequate for design purposes.

The effect of heat transfer between the vapor and liquid phases was examined by Liang and Smith (22), using a small packed column and an inverted pear column. The investigated binary systems were acetone-benzene, carbon tetrachloride-toluene and acetone-chloroform. The graph of H_{OG} versus $\frac{1}{2}(y_{AO}+y_{AT})$, measured in the packed column, appears to have the same trends as those of Sawistowski and Smith (30) and Quershi and Smith (27). The results for the carbon tetrachloride-toluene and acetone-chloroform mixtures did not agree with the results of Sawistowski and Smith (30) for the same systems. The resulting curves of Liang and Smith (22) for N_{OG} versus $\frac{1}{2}(y_{AO}+y_{AT})$ increased with the increase in the more volatile component without even reaching a maximum value. The efficiency of a distillation column should reach a maximum and become smaller as the concentration of the more volatile component approaches one. This is predicted by both theoretical and experimental results of all other investigations. The data were also very scattered.

The bottom liquid composition sample was taken at the center of the base of the packing. The scattering of the data may be partially explained by the fact that the liquid stream did not have a chance to mix well. The authors derived a set of equations based on heat and mass balances for a differential height of the packed column. The equations were solved for constant values of heat and mass transfer coefficients. The authors compared their data with the derived equations and found the behavior at the end points was unusual. They found that the heat transfer due to the condensation of the more volatile component was much less than the heat transfer due to the temperature difference between the phases in the range where $\frac{1}{2}(y_{AO}+y_{AT})$ approaches one. Since there is a very small temperature difference between the vapor and the liquid in this range, one would normally expect the thermal distillation effects to be minor. The reported results may also be in error due to the sampling technique used. The equations derived by the authors assumed that all of the changes in the vapor flow rate were due to thermal distillation and that none of the changes were due to the difference in the latent heats of vaporization or that required to maintain the liquid at its saturation temperature. It will be shown later that these should be considered.

Hochgesand (16) stated it was necessary to know where the major part of the resistance to mass transfer exists, in the liquid or the vapor, before the interfacial composition would be known and

before a model could be used to predict the behavior of the system. The benzene-n-hexane mixture was investigated. This system has a relative volatility of less than 1.5. In the investigated composition range, the vapor-liquid equilibrium line was a straight line with a known slope. The flashing-mixing effect would be small for this system and the temperature difference between the vapor and the liquid would not be very large; accordingly, thermal effects would not be very significant for this system. The wetted-wall column was surrounded by a heat transfer liquid to produce vaporization or condensation. The author found that the number of transfer units, N_{OG}, decreased as the amount of condensation increased. The main purpose of the heat transfer investigation was to show that almost all of the resistance to mass transfer was on the vapor side of the vapor-liquid interface and that the liquid resistance was negligible. The temperature difference, which was considered, was between the temperature of the vapor and the liquid outside the wetted-wall column. For example, the temperature difference was zero when the vapor temperature was equal to the bath temperature. For thermal effect studies, the temperature difference that should be considered is between the liquid on the inside wall and the surrounding bath material. When they are equal, the net heat transfer will be zero. The author showed that since the major resistance to heat transfer was in the vapor phase, the mass transfer could be described by Whitman's two-film theory (33).

Thermal gradients were not considered in the resulting equations.

Everitt and Hutchison (11) investigated the four binary systems acetone-benzene, ethanol-water, ethanol-benzene and isopropanol-water. The authors used a wetted-wall column to investigate the systems. The experimental data were used to calculate the number of transfer units, N_{OG}, using Equation (1). The values of N_{OG} were plotted versus $\frac{1}{2}(y_{AO}+y_{AT})$. The results for the actone-benzene mixture did not match the results obtained by Quershi and Smith (27) is a wetted-wall column. The acetone-benzene results did not show much variation with composition, whereas the results of Quershi and Smith (27) varied greatly over the same composition range. Measurements for ethanol-water were taken only for a few compositions, not enough to adequately describe the dependency. The results for ethanol-water and isopropanol-water showed the same type of variation for an azeotrope as did Liang and Smith (22); unfortunately the experimental trend was ignored in favor of their theoretical results. The authors concluded that their theoretical calculations showed a significant liquid-side resistance existing for distillation. The values for the mass transfer coefficients were calculated from the results of Hatta (13) for the liquid-side and Gilliland and Sherwood (12) for the vapor-side. It was noted by the authors that the equations of Hatta (13) was not directly applicable to long wetted-wall columns, so modifications were necessary. The authors reasoned

that the number of transfer units, N_{OG}, should not go to zero as the composition goes to zero or one but should remain a finite number greater than zero. Although the resulting theory agrees well with the acetone-benzene mixture data, it completely ignores trends found in the data of the other three systems. It should also be noted that the experimental data for the only mixture which does agree with their theory are in conflict with the data of Quershi and Smith (27), as previously mentioned.

Hutchison and Lusis (17) examined the performance of four binary-mixtures in a wetted-wall column. The systems were benzene-toluene, cyclohexane-toluene, methyl ethyl ketone-toluene and isopropanol-toluene. The experimental results were used to calculate the number of transfer units, N_{OG}, by Equation (1). These results were compared with the values of N_{OG} based on mass transfer coefficients calculated from analogy equations. The liquid phase equation was that of Hakita, Nakanishi and Kataoka (14) and the vapor phase equation was that of Gilliland and Sherwood (12). The experimental results generally showed the same trends near the end points as was shown by Quershi and Smith (27) and Sawistowski and Smith (30). The end-point trends were ignored in favor of the same conclusions as Everitt and Hutchison (11). However, the authors did point out that the liquid side resistance was less than 15 percent of the total resistance, much less than was found by Everitt and

Hutchison (11). The resulting curves did approximate the performance in certain concentration ranges but did not account for the overall variations or end-point trends.

It is interesting to note that the concentration range with the best agreement between experimental results and results predicted by the two-film method is in the intermediate composition range. This is the range which would most likely have the greatest variation due to thermal effects. This agreement is most likely due to the fact that the coefficients are calculated to fit experimental data. However, since the thermal effects are different for each system, the equations could not possibly fit all systems.

A means of calculating the number of transfer units as a function of both the concentration driving force as in Equation (1) and the thermal effects would be needed to be able to apply it to all systems. An equation of this type will be developed and discussed.

PRESENTATION OF PRESENT THEORY

When formulating a valid model which describes the actual amount of mass transfer taking place, all driving forces which might exist must be examined. The usual method is to consider the concentration difference between the interface and the bulk phase as the only driving force of importance. Because of differences between predicted results and experimental results, it is necessary to evaluate other driving forces. The additional driving force which must be examined is the temperature difference between the liquid and the vapor phases.

In deriving the model, the control volume for the vapor will be the vapor space between the axis of the column and the vapor-liquid interface as shown in Figure 2. This space is bounded at z and $z + dz$. The control volume for the liquid is bounded on the sides by the vapor-liquid interface and the tube wall and bounded on the bottom and top by z and $z + dz$ respectively. In the following balances, A will be used to designate the more volatile component with a net flux from the liquid to the vapor and B will designate the less volatile component with a net flux from the vapor to the liquid. The complete energy balance on the vapor phase will first be derived; this balance will be related later to the liquid phase energy balance and the mass balance on component A. The following terms relate the

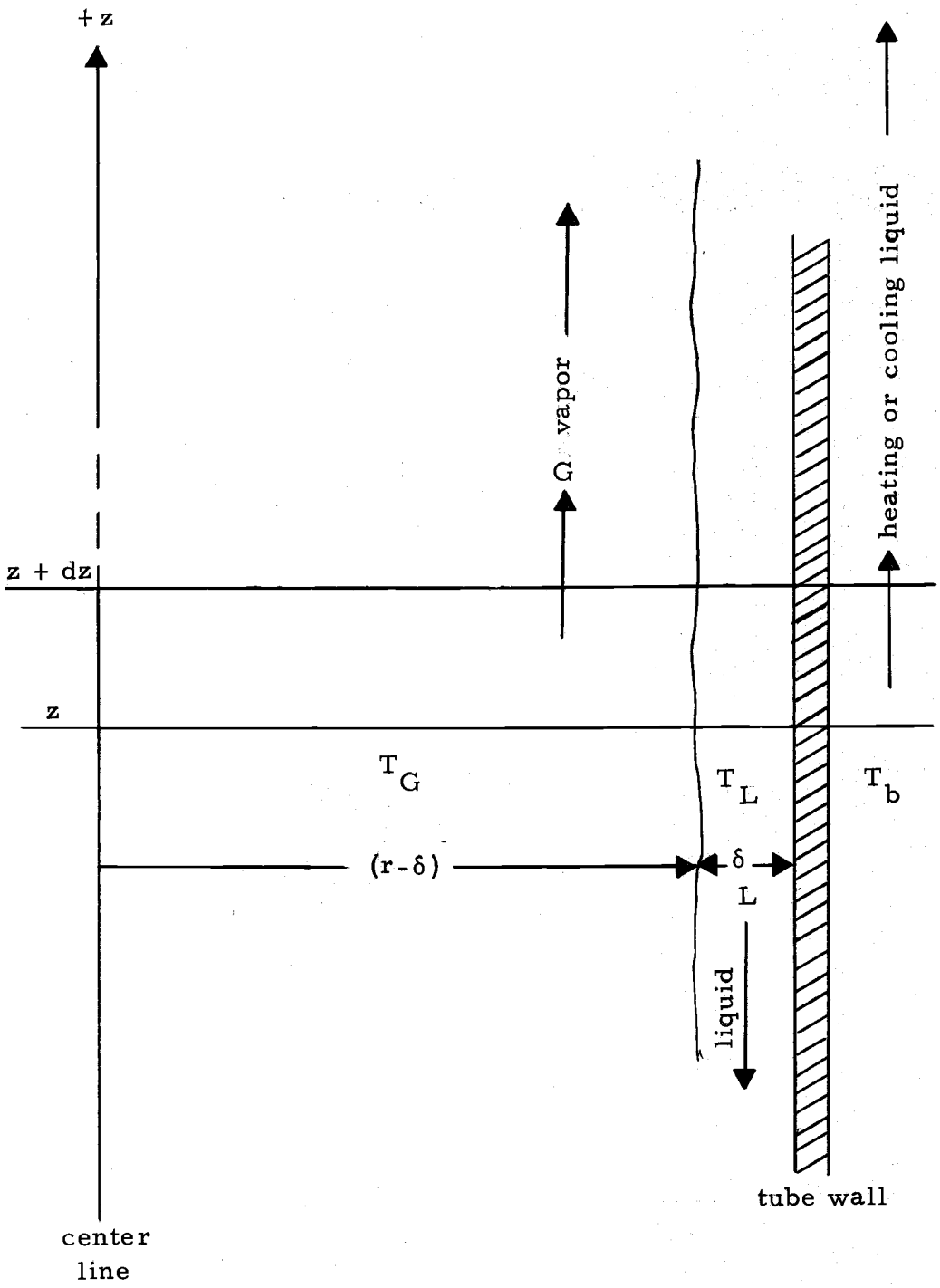

Figure 2. Control volume of the column.

energy transferred into the control volume and out of the control volume. The accumulation term will be zero since the system will be assumed to be at steady-state and the heat of mixing in vapor will be negligible. In the following equation $\vec{N}_A$ will be used to symbolize the r-component of the flux of component A.

In: $$(GH_G)\Big|_z \pi(r-\delta)^2 - (\vec{N}_A\lambda_A + \vec{N}_A h_A)_i 2\pi(r-\delta)dz$$

Out: $$(GH_G)\Big|_{z+dz} \pi(r-\delta)^2 + \{(\vec{N}_B\lambda_B + \vec{N}_B h_B)_i + h_V(T_G - T_i)\}2\pi(r-\delta)dz$$

Accumulation: 0 (steady state)

accumulation = input - output

or

input = output

Also one may make the assumption after taking the limit as Δz approaches zero

$$(GH_G)\Big|_{z+dz} = (GH_G)\Big|_z + \frac{d}{dz}(GH_G)\Big|_z dz$$

then

$$(GH_G)\Big|_z \pi(r-\delta)^2 - (\vec{N}_A\lambda_A + \vec{N}_A h_A)_i 2\pi(r-\delta)dz$$

$$= (GH_G)\Big|_z \pi(r-\delta)^2 + \pi(r-\delta)^2 \frac{d}{dz}(GH_G)\Big|_z dz$$

$$+ \{(\vec{N}_B\lambda_B + \vec{N}_B h_B)_i + 2h_V(T_G - T_i)\}\pi(r-\delta)dz \qquad (3)$$

Cancelling the terms which appear on both sides of Equation (3), Equation (4) results.

$$-\frac{d}{dz}(GH_G) = \frac{2}{(r-\delta)}\left[\vec{N}_B\lambda_B+\vec{N}_A\lambda_A+\vec{N}_Bh_B+\vec{N}_Ah_A\right]_i + \frac{2h_V(T_G-T_i)}{(r-\delta)} \quad (4)$$

The analogous energy balance will now be derived for the liquid phase.

In: $2\pi r\delta(H_L L)\Big|_z + [h_V(T_G-T_i)+(\vec{N}_B\lambda_B+\vec{N}_Bh_B)_i]2\pi(r-\delta)dz$

Out: $2\pi r\delta(H_L L)\Big|_{z+dz} + h_b(T_L-T_b)2\pi r dz - [(\vec{N}_A\lambda_A+\vec{N}_Ah_A)_i]2\pi(r-\delta)dz$

Accumulation: 0 (steady state)

or as before

$$\text{input} = \text{output}$$

and after taking the limit as Δz approaches zero.

$$(H_L L)\Big|_{z+dz} = (H_L L)\Big|_z + \frac{d}{dz}(H_L L)\Big|_z dz$$

$$2\pi r\delta(LH_L)\Big|_z + [h_V(T_G-T_i)+(\vec{N}_B\lambda_B+\vec{N}_Bh_B)_i]2\pi(r-\delta)dz$$

$$= 2\pi r\delta(LH_L)\Big|_z - [\vec{N}_A\lambda_A+\vec{N}_Ah_A]_i 2\pi(r-\delta)dz + h_b(T_L-T_b)2\pi r dz$$

$$+ 2\pi r\delta\frac{d}{dz}(LH_L)dz \quad (5)$$

Cancelling the terms which appear on both sides of Equation (5), Equation (6) results.

$$-\frac{d}{dz}(LH_L) = \frac{h_b(T_L-T_b)}{\delta} - \frac{(r-\delta)}{r\delta}\left[h_V(T_G-T_i)+(\vec{N}_A\lambda_A+\vec{N}_Bh_B+\vec{N}_Ah_A+\vec{N}_B\lambda_B)_i\right] \quad (6)$$

The next step will be to derive the equation describing the transfer of component A into the vapor phase. The first term to be defined will be the term which accounts for the amount of A transferred due to the concentration driving force.

$$-\vec{N}'_A = K'_G a(y^*_A - y_A) \tag{7}$$

The amount of A vaporized due to the concentration difference defines the amount of B which condenses due to the concentration difference by the energy balance shown in Equation (8).

$$N'_A \lambda_{Ai} + N'_B \lambda_{Bi} = 0 \tag{8}$$

The next term to be defined will be the amount of A vaporized due to the heat transferred from the vapor to the liquid because of the temperature difference. The energy transferred will vaporize both A and B since this is the same as adding energy to a boiling liquid. The amount of A vaporized will be given by the product of the vapor mole fraction of A at the vapor-liquid interface and the total moles of A and B vaporized.

$$\frac{y_{Ai}}{\lambda_{mi}} h_V (T_G - T_i) \tag{9}$$

The amount of A vaporized due to the heat transferred from the

fluid surrounding the column will be Equation (10).

$$\frac{y_{Ai}}{\lambda_{mi}} h_b(T_b - T_L) \tag{10}$$

The energy supplied to the liquid by condensing B, which is in excess or in deficit as required by Equation (8), will vaporize the amount of A given in Equation (11).

$$(\vec{N}'_B - \vec{N}_B)(\lambda_{Bi}/\lambda_{Ai}) \tag{11}$$

If the system is non-ideal where the heat of mixing term becomes important, Equation (12) is needed. This term gives the amount of A which would or would not vaporize due to the heat of mixing requirements.

$$-\frac{1}{\lambda_{Ai}} \frac{d}{dz} (L\Delta H_m)dz \tag{12}$$

The last term to be considered will be due to the energy required to maintain the liquid at the saturation temperature.

$$\frac{1}{\lambda_{Ai}} \frac{d}{dz} \{LC_{PL}(T - T_{ref})\}dz \tag{13}$$

The total A transferred into the vapor phase will include all of these terms and is given by Equation (14).

$$\pi(r-\delta)^2 d(Gy_A) = \pi(r-\delta)^2 K'_G a(y_A^* - y_A)dz$$
$$+ (\vec{N}'_B - \vec{N}_B)(\lambda_{Bi}/\lambda_{Ai})2\pi(r-\delta)dz$$
$$+ \frac{y_{Ai}}{\lambda_{mi}} \{2\pi(r-\delta)dzh_V(T_G - T_i) + 2\pi r dz h_b(T_b - T_L)\}$$
$$+ \frac{2\pi r\delta}{\lambda_{Ai}} \{\frac{d}{dz}[LC_{PL}(T-T_{ref})] - \frac{d}{dz}(L\Delta H_m)\}dz \qquad (14)$$

Cancelling the terms which appear on both sides of Equation (14), it simplifies to Equation (15).

$$\frac{d}{dz}(Gy_A) = K'_G a(y_A^* - y_A) + \frac{2\lambda_{Bi}}{(r-\delta)\lambda_{Ai}}(\vec{N}'_B - \vec{N}_B) - \frac{2r\delta}{\lambda_{Ai}(r-\delta)^2}\frac{d}{dz}(L\Delta H_m)$$
$$+ \frac{2y_{Ai}}{(r-\delta)\lambda_{mi}} \{h_V(T_G - T_L) + \frac{rh_b}{(r-\delta)}(T_b - T_L)\}$$
$$+ \frac{2r\delta}{(r-\delta)^2\lambda_{Ai}} \{\frac{d}{dz}(LC_{PL}(T-T_{ref})\} \qquad (15)$$

For the sake of simplicity let the following definition be made.

$$\theta = \frac{2\lambda_{Bi}}{(r-\delta)\lambda_{Ai}}(\vec{N}'_B - \vec{N}_B) - \frac{2r\delta}{\lambda_{Ai}(r-\delta)^2}\frac{d}{dz}(L\Delta H_m)$$
$$+ \frac{2r\delta}{\lambda_{Ai}(r-\delta)^2}\frac{d}{dz}[LC_{PL}(T-T_{ref})] + \frac{2y_{Ai}}{\lambda_{mi}(r-\delta)}\{h_V(T_G - T_i) + \frac{rh_b}{(r-\delta)}(T_b - T_L)\} \qquad (16)$$

The abbreviated form of Equation (14) becomes Equation (16).

$$\frac{d}{dz}(Gy_A) = K'_G a(y_A^* - y_A) + \theta \tag{17}$$

$$G\frac{dy_A}{dz} = -y_A\frac{dG}{dz} + K'_G a(y_A^* - y_A) + \theta \tag{18}$$

Equation (4) then can be put in the same form as Equation (18).

$$-H_G\frac{dG}{dz} = G\frac{dH_G}{dz} + \frac{2}{(r-\delta)}\left[\vec{N}_B\lambda_B + \vec{N}_A\lambda_A + \vec{N}_B h_B + \vec{N}_A h_A\right]_i + \frac{2h_V(T_G - T_i)}{(r-\delta)} \tag{19}$$

Equations (18) and (19) can be used to eliminate the term dG/dz.

$$G\frac{dy_A}{dz} = K'_G a(y_A^* - y_A) + \theta + \frac{y_A G}{H_G}\frac{dH_G}{dz} + \frac{y_A}{H_G}\left\{\frac{2}{(r-\delta)}\left[\vec{N}_B\lambda_B + \vec{N}_A\lambda_A + \vec{N}_B h_B + \vec{N}_A h_A\right]_i + \frac{2y_{Ah_V}(T_G - T_i)}{(r-\delta)H_G}\right\} \tag{20}$$

If the system is operating at total reflux, the equation may be simplified since the mass flow rate in the vapor phase is equal to the mass flow rate in the liquid phase, but in the opposite direction.

$$\pi(r-\delta)^2 G = -2\pi r\delta L$$

$$-L = \frac{(r-\delta)}{2r\delta}G$$

but

$$-\frac{dL}{dz} = \frac{(r-\delta)}{2r\delta}\frac{dG}{dz} \tag{21}$$

Upon the rearrangement of Equation (6)

$$-H_L \frac{dL}{dz} = +L \frac{dH_L}{dz} - \frac{h_b}{\delta}(T_b - T_L)$$

$$- \frac{(r-\delta)}{r\delta}[h_V(T_G - T_i) + (\vec{N}_A\lambda_A + \vec{N}_B\lambda_B + \vec{N}_A h_A + \vec{N}_B h_B)_i] \quad (22)$$

and substitution of Equation (21) into (22), one obtains

$$H_L \frac{dG}{dz} = -G \frac{dH_L}{dz} + \frac{2rh_b(T_b - T_L)}{(r-\delta)^2}$$

$$- \frac{2}{(r-\delta)}[h_V(T_G - T_i) + (\vec{N}_A\lambda_A + \vec{N}_B\lambda_B + \vec{N}_A h_A + \vec{N}_B h_B)_i] \quad (23)$$

Eliminating $\frac{dG}{dz}$ from Equations (18) and (23), Equation (24) results.

$$G\frac{dy_A}{dz} = K_G a(y_A^* - y_A) + \theta + \frac{y_{AG}}{H_L}\frac{dH_L}{dz} - \frac{2rh_b(T_b - T_L)y_A}{(r-\delta)^2 H_L}$$

$$+ \frac{2y_A}{H_L(r-\delta)}[h_V(T_G - T_i) + (\vec{N}_A\lambda_A \vec{N}_B\lambda_B + \vec{N}_A h_A + \vec{N}_B h_B)_i] \quad (24)$$

If Equation (20) is multiplied by H_G and Equation (24) is multiplied by H_L, Equation (24) can be subtracted from Equation (20) to eliminate a term which would otherwise be difficult to evaluate.

$$G\frac{dy_A}{dz} = K'_G a(y_A^* - y_A) + \theta + \frac{y_A G}{(H_G - H_L)}\frac{d(H_G - H_L)}{dz} - \frac{2y_A rh_b(T_b - T_L)}{(r-\delta)^2(H_G - H_L)} \quad (25)$$

Substituting the complete form of θ as given in Equation (16) and rearranging, the complete Equation (26) results.

$$G\frac{dy_A}{dz} = K'_G a(y_A^* - y_A) + \left\{ \frac{2\lambda_{Bi}}{(r-\delta)\lambda_{Ai}}(N'_B - N_B) + \frac{2y_{Ai}h_V}{(r-\delta)\lambda_{mi}}(T_G - T_L) \right.$$
$$+ \frac{1}{\lambda_{Ai}}\frac{d}{dz}(GC_{PL}(T-T_{ref})) + \frac{y_A G}{(H_G-H_L)}\frac{d(H_G-H_L)}{dz}$$
$$\left. - \frac{1}{\lambda_{Ai}}\frac{d}{dz}(G\Delta H_m) \right\} + \frac{2rh_b}{(r-\delta)^2}(T_b - T_L)\left\{ \frac{y_{Ai}}{\lambda_{mi}} - \frac{y_A}{(H_G-H_L)} \right\} \quad (26)$$

For easier handling of the equations, definitions will be made for the terms in the brackets. The first term, $\phi(y_A, y_{Ai})$, is defined by

$$\phi(y_A, y_{Ai}) = \frac{1}{K'_G a}\left[\frac{2\lambda_{Bi}}{(r-\delta)\lambda_{Ai}}(\vec{N}'_B - \vec{N}_B) + \frac{2y_{Ai}h_V(T_G - T_i)}{(r-\delta)\lambda_{mi}} \right.$$
$$+ \frac{1}{\lambda_{Ai}}\frac{d}{dz}(GC_{PL}(T-T_{ref})) - \frac{y_A G}{(H_G-H_L)}\frac{d(H_G-H_L)}{dz}$$
$$\left. - \frac{1}{\lambda_{Ai}}\frac{d}{dz}(G\Delta H_m) \right] \quad (27)$$

The composition in the vapor, y_A, sets the vapor temperature and the enthalpy per unit mass of mixture of the vapor, H_G. Since the column is operating at total reflux, x_A equals y_A at any point in the column. This establishes the composition, saturation temperature and the enthalpy per unit mass of solution, H_L. The composition

at the vapor-liquid interface, y_{Ai}, defines the saturation temperature, T_i, and in turn defines all of the physical properties. The second term is defined by

$$\phi'(y_A, y_{Ai}, T_b) = \frac{1}{K'_G a}\left[\frac{2rh_b(T_b - T_L)}{(r-\delta)^2}\left\{\frac{y_{Ai}}{\lambda_{mi}} - \frac{y_A}{(H_G - H_L)}\right\}\right] \qquad (28)$$

The liquid-vapor interface composition also defines the interfacial temperature, T_i, and the latent heat of vaporization of the mixture, λ_{mi}. The bulk vapor composition y_A defines the saturated vapor temperature, T_G, the liquid composition, x_A, and the enthalpy per unit mass of mixture for both the liquid and vapor. The bath temperature T_b can be independently controlled so it must be considered a variable. Using the definitions given by Equations (27) and (28) in Equation (26), the generalized Equation (29) results.

$$G\frac{dy_A}{dz} = K'_G a\left[(y_A^* - y_A) + \phi(y_A, y_{Ai}) + \phi'(y_A, y_{Ai}, T_b)\right] \qquad (29)$$

Equation (29) can now be separated and integrated between the appropriate limits:

$$\text{at} \quad z = 0 \qquad y_A = y_{AO}$$

$$\text{at} \quad z = z \qquad y_A = y_{AT}$$

$$z = \int_0^z dz = \int_{y_{AO}}^{y_{AT}} \frac{G dy_A}{K'_G a\{(y_A^* - y_A) + \phi(y_A, y_{Ai}) + \phi'(y_A, y_{Ai}, T_b)\}} \qquad (30)$$

For the case where $(G/K'_G a)$ is essentially independent of composition, y_A, over a short composition range, Equation (30) can be put in the form of Equation (31).

$$z = \left(\frac{G}{K'_G a}\right) \int_{y_{AO}}^{y_{AT}} \frac{dy_A}{(y_A^* - y_A) + \phi(y_A, y_{Ai}) + \phi'(y_A, y_{Ai}, T_b)} \qquad (31)$$

By analogy to the original definition of the number of transfer units, N_{OG}, given in Equation (1), the modified form N'_{OG} is then given by Equation (32).

$$N'_{OG} = \int_{y_{AO}}^{y_{AT}} \frac{dy_A}{(y_A^* - y_A) + \phi(y_A, y_{Ai}) + \phi'(y_A, y_{Ai}, T_b)} \qquad (32)$$

By analogy to the height of a transfer unit, H_{OG}, given in Equation (1), a modified definition of the height of a transfer unit, H'_{OG}, is given by Equation (33).

$$H'_{OG} = \frac{G}{K'_G a} \qquad (33)$$

The effect of $\phi(y_A, y_{Ai})$ and $\phi'(y_A, y_{Ai}, T_b)$ need to be examined relative to both Equations (1) and Equation (32).

DISCUSSION OF PRESENT THEORY

The usual assumption which is made in calculating the efficiency of a continuous contact distillation column is that the concentration difference between the phases is the only driving force for mass transfer. For the purpose of comparison the mass transfer equation based on this assumption will be derived here using the nomenclature used in the previous sections.

The amount of mass transfer which takes place in a differential height dz of the column is

$$d(Gy_A) = K_G a(y_A^* - y_A)dz \tag{34}$$

If the additional assumption is made that G is constant throughout the entire column, then

$$Gdy_A = K_G a(y_A^* - y_A)dz. \tag{35}$$

After separating the variables, the equation is integrated between the appropriate limits.

$$z = \int_0^z dz = \int_{y_{AO}}^{y_{AT}} \frac{Gdy_A}{K_G a(y_A^* - y_A)} \tag{36}$$

The next step is to assume that the term $\frac{G}{K_G a}$ is constant over the given composition range.

$$z = \left(\frac{G}{K_G a}\right) \int_{y_{AO}}^{y_{AT}} \frac{dy_A}{(y_A - y_A^*)} \tag{37}$$

The two terms on the right side have been defined by Chilton and Colburn (4),

$$N_{OG} = \int_{y_{AO}}^{y_{AT}} \frac{dy_A}{(y_A - y_A^*)} \tag{1}$$

and

$$H_{OG} = (G/K_G a) \tag{2}$$

These definitions serve adequately for gas absorption operations where the absorbed component is very dilute and it is carried in an inert carrier gas. For the case where the absorbed component is not dilute, corrections must be made for G and $K_G a$. Equations (1) and (2) are applied directly to distillation processes where the components are not dilute and large amounts of energy are exchanged. The effect of this exchange of energy in the various forms is considered in the present work.

If one compared Equations (1) and (2) with experimental data taken in a column of fixed height, the product of N_{OG} and H_{OG} must be a constant. In addition, if the assumption $(G/K_G a)$ equals a constant is true, then obviously the term

$$N_{OG} = \int_{y_{AO}}^{y_{AT}} \frac{dy_A}{(y_A^* - y_A)} \qquad (1)$$

must be constant for the entire composition range. However, it has been shown by several previous authors (10, 17, 22, 27, 29) that N_{OG} varied with respect to $\frac{1}{2}(y_{AO}+y_{AT})$ as shown in Figure 3. The experimental data were taken in various types of packed columns and wetted-wall columns. It has been shown (33) that the value of K_G depends on the physical properties of the two phases, the slope of the vapor-liquid equilibrium curve and the mass flow rates of the two phases. Sawistowski and Smith (30) found that the variation in these terms could not account for all the variation in N_{OG} which was experimentally observed. The authors concluded that the thermal effects which existed needed to be considered.

To explain the additional variation a phenomenon termed "thermal distillation" was postulated. It was shown in the present theory what additional terms were involved in the thermal effect. For the discussion of the thermal influence the definitions of $\phi(y_A, y_{Ai})$ and $\phi'(y_A, y_{Ai}, T_b)$ are given by Equations (27) and (28), respectively. Using these terms the modified form of the equation is Equation (32).

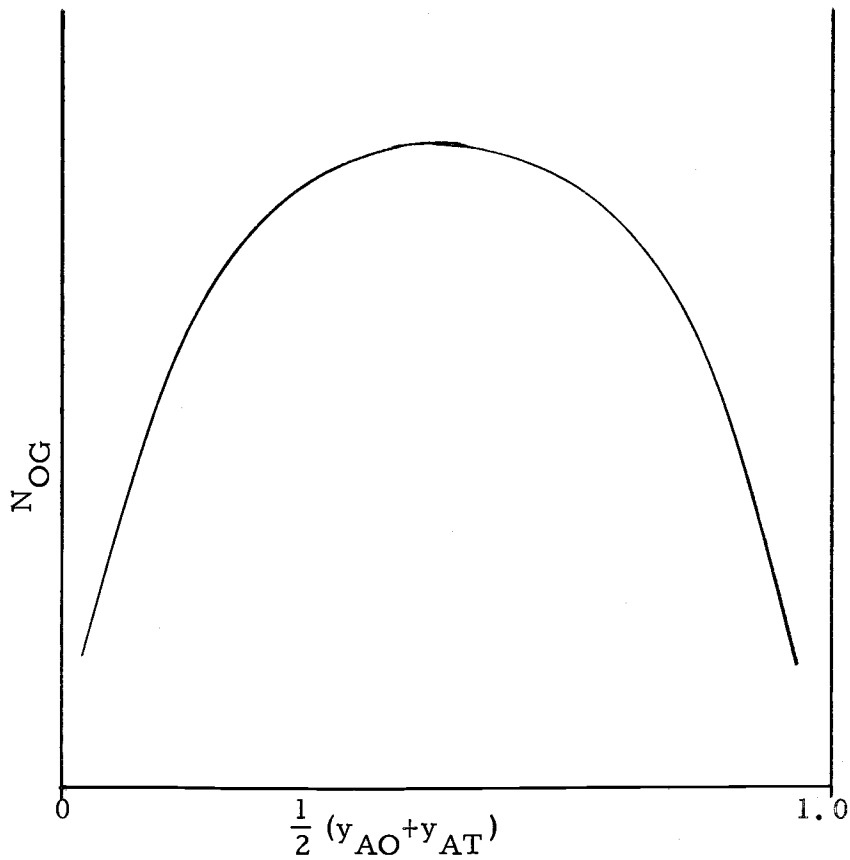

Figure 3. Typical variation of N_{OG} with the average composition in the continuous contact equipment.

$$N'_{OG} = \int_{y_{AO}}^{y_{AT}} \frac{dy_A}{(y_A^* - y_A) + \phi(y_A, y_{Ai}) + \phi'(y_A, y_{Ai}, T_b)} \qquad (32)$$

The shaded area shown in Figure 4 will be the value of N_{OG} as defined by Equation (1).

The effect of the thermal term will now be examined relative to the performance of an adiabatic, fixed height, wetted-wall column operating at total reflux. Under adiabatic conditions, $\phi'(y_A, y_{Ai}, T_b)$ is zero. When the difference between y_{AO} and y_{AT} is not large, G will not change significantly and K_G, which varies as G and depends on physical properties, will also remain essentially constant. Therefore, the value of G/K_Ga will be very close to a constant. If G/K_Ga is a constant, then N'_{OG} must also remain constant.

If the value of $\phi(y_A, y_{Ai})$ is greater than zero, then the value of $1/\{(y_A^* - y_A) + \phi(y_A, y_{Ai})\}$ will become smaller as the value of $\phi(y_A, y_{Ai})$ increases. For the value of N'_{OG} to remain constant, the value of y_{AT} will need to increase for a given inlet composition y_{AO}. Correspondingly, if the value of $\phi(y_A, y_{Ai})$ is less than zero, the value of y_{AT} will have to decrease for the value of N'_{OG} to remain the same.

Under non-adiabatic conditions, $\phi'(y_A, y_{Ai}, T_b) \neq 0$, the reasoning should be the same for positive and negative values of

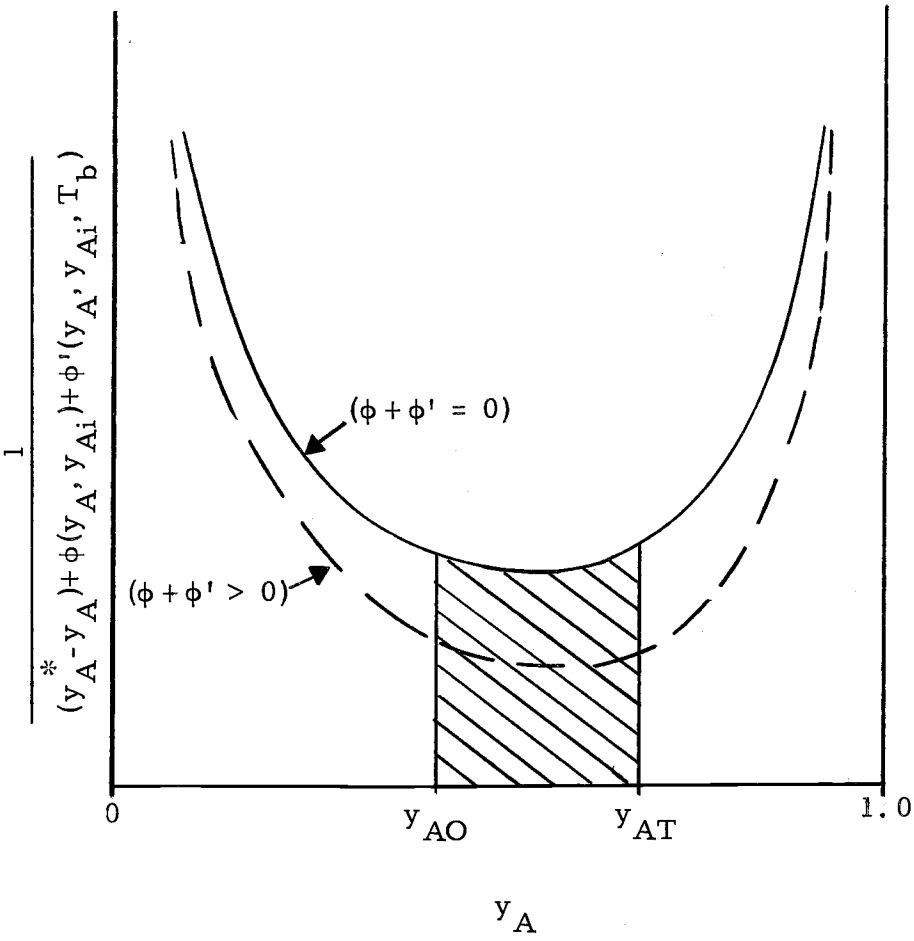

Figure 4. Integration of Equation (32).

$\phi'(y_A, y_{Ai}, T_b)$ as for $\phi(y_A, y_{Ai})$. One would conclude from this that by varying $\phi'(y_A, y_{Ai}, T_b)$ under experimental conditions, the influence would be analogous to the influence of $\phi(y_A, y_{Ai})$.

As a result of the above arguments, the maximum in N_{OG} versus $\frac{1}{2}(y_{AO} + y_{AT})$ can be explained. The difference $(y_{AT} - y_{AO})$ has been increased by the thermal effects, but the influence of the thermal term in the driving force has been ignored when evaluating N_{OG}. Since the thermal term, under adiabatic conditions, would be a maximum at an intermediate composition, it is obvious the increase in $(y_{AT} - y_{AO})$ will be a maximum. Thus the increase in N_{OG} will be a maximum.

Danckwerts, Sawistowski and Smith (8) suggested the relative volatility could be an important factor in thermal distillation. This theory is substantiated by Equation (32). The higher the relative volatility, the larger the temperature difference between the two phases will be. In addition, the term in $\phi(y_A, y_{Ai})$ that is a product of y_{Ai} is always positive and the term that is a product of y_A is generally negative. Since the magnitude of y_{Ai} relative to y_A is dependent on the relative volatility, it can be concluded that the higher the relative volatility, the more important the thermal effect.

DESCRIPTION OF EQUIPMENT

The design of the wetted-wall column system, although similar to that used by Quershi and Smith (27), included a number of modifications made either to simplify operation or to provide better performance. The wetted-wall column and associated equipment are illustrated in the schematic drawing of the apparatus in Figure 5.

The column was made of pyrex glass tubing which had a length of 122 cm and an outside diameter of 2. 54 cm. The top edge of the column was ground to a sharp knife-edge, and the edge was perpendicular to the vertical axis of the column. The bottom of the column was widened into a bell with a 5. 0 cm diameter so that the column would fit closely over the vapor inlet to the column. The column was sealed into the lower liquid chamber by a standard taper joint.

The upper chamber had a liquid volumn of 95 cm^3 while the lower chamber had a liquid volume of 110 cm^3. These small volumes were advantageous since the residence time in each chamber was less than one minute. The rate at which the liquid left the lower chamber was controlled with a 4 mm bore stopcock. The vapor exit from the upper chamber was sealed by the use of a standard taper joint. Illustrations of the chambers, bells and knife edge appear in Figures 6, 7, 8 and 9.

The boiling vessel was fabricated from an eight-liter, stainless

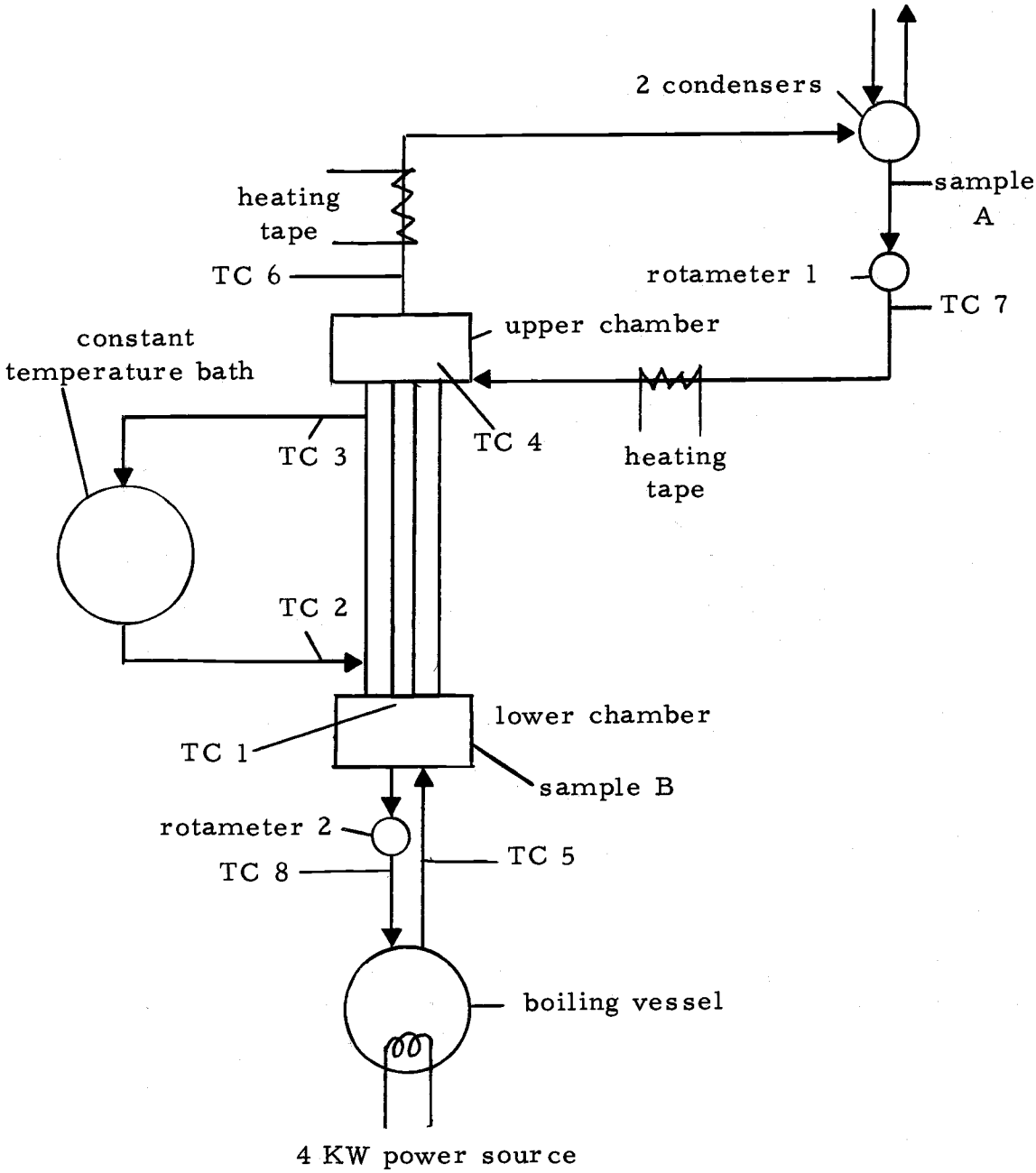

Figure 5. Schematic of entire system.

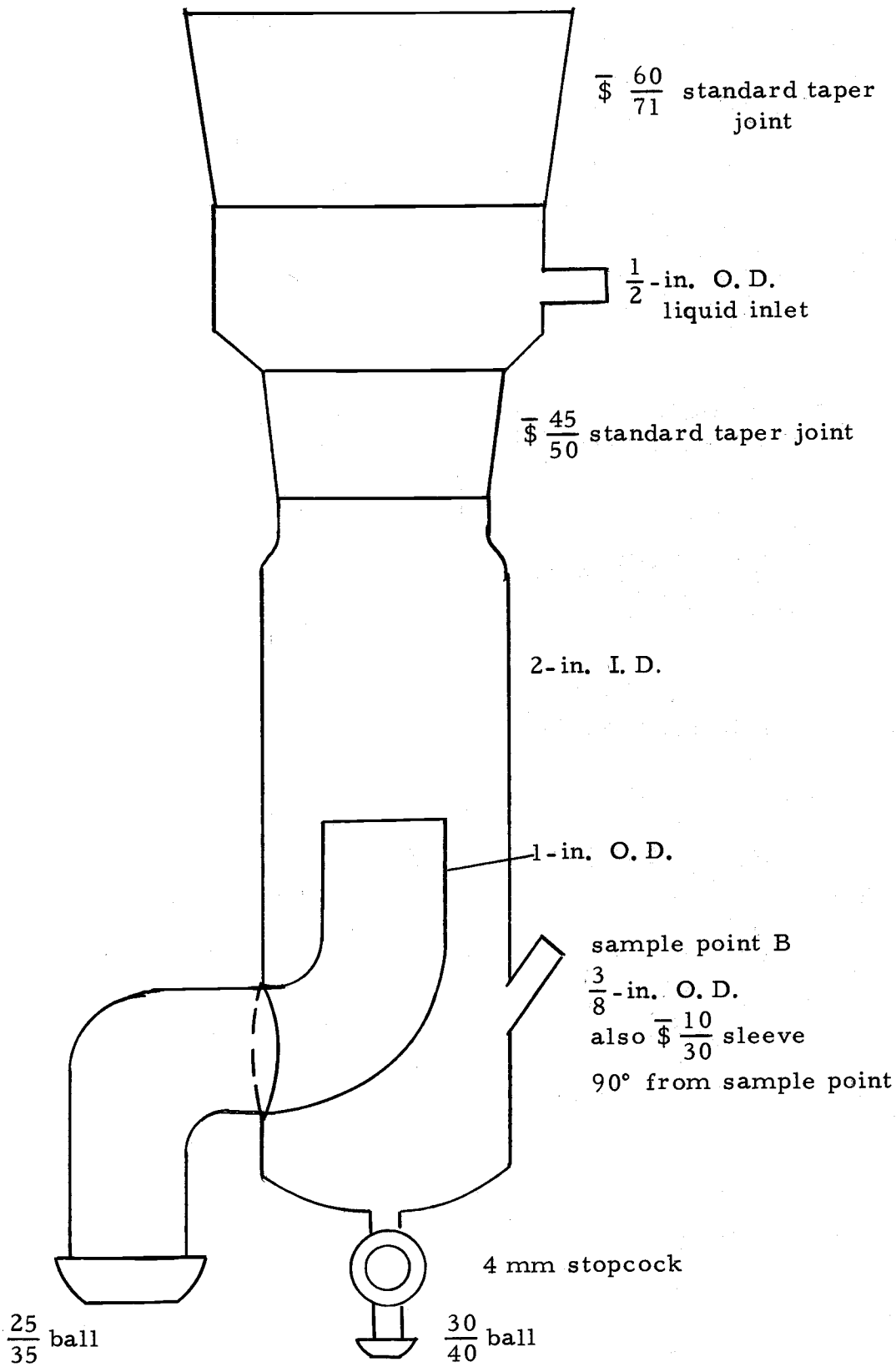

Figure 6. Diagram of lower chamber.

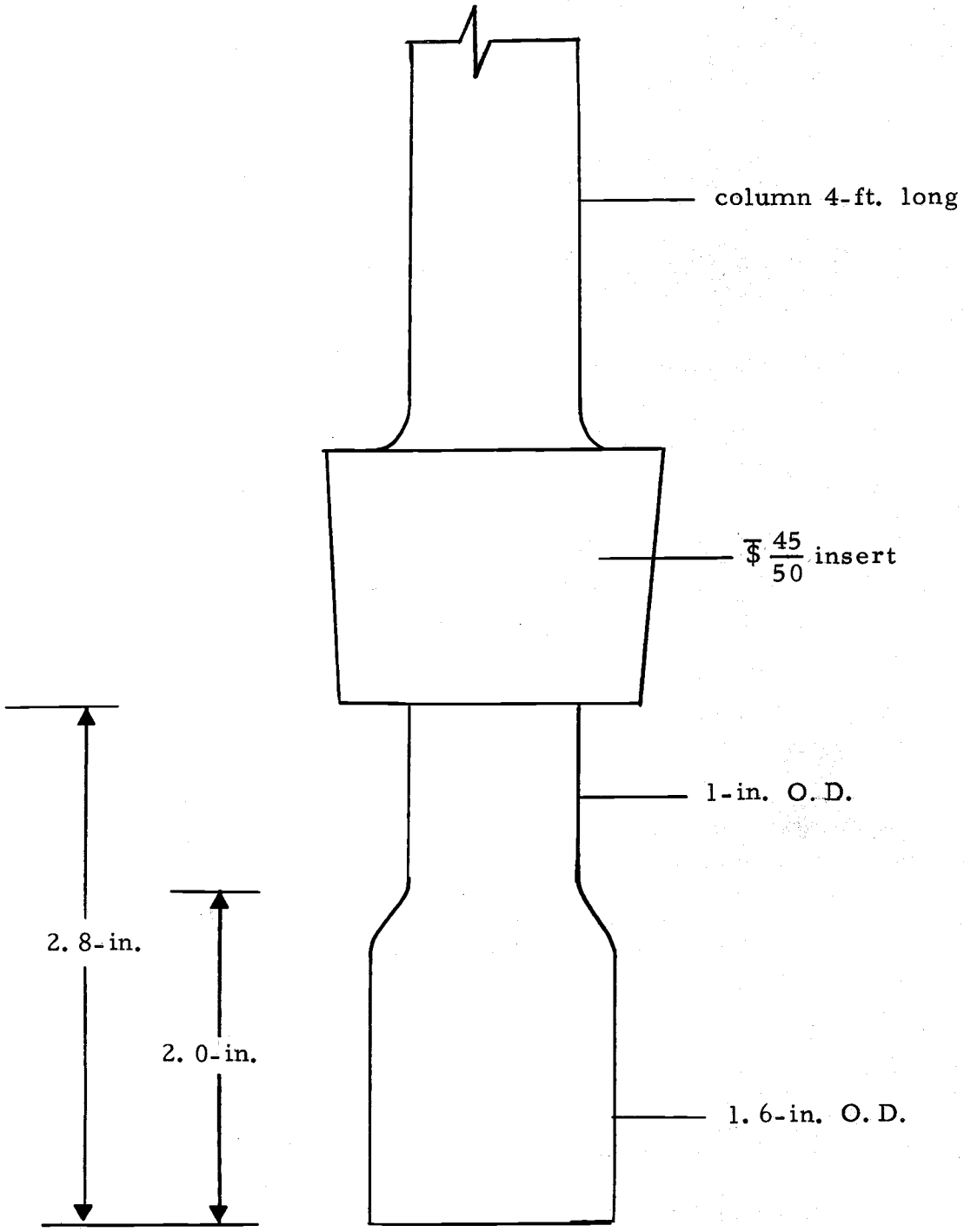

Figure 7. Bell of lower chamber.

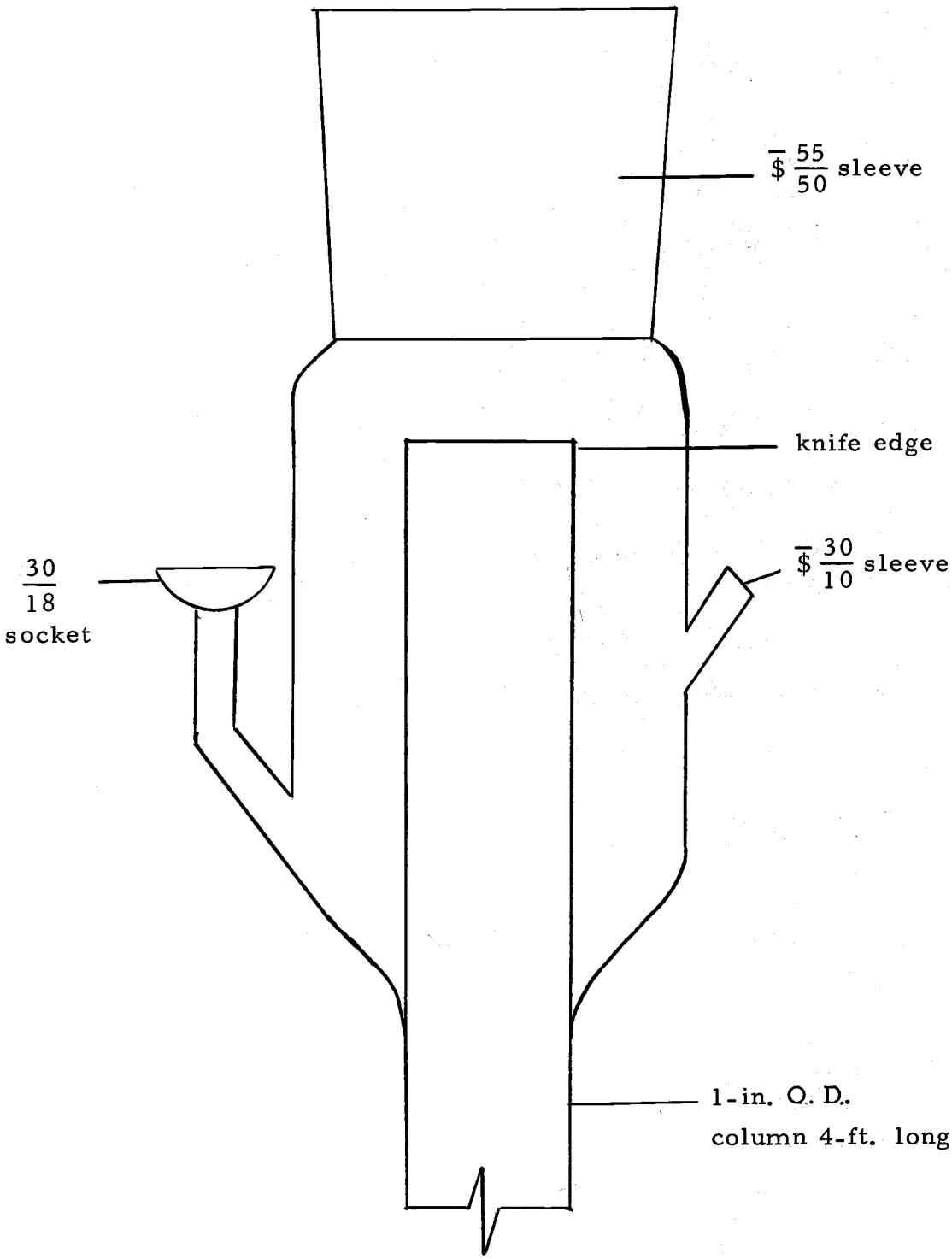

Figure 8. Diagram of upper chamber.

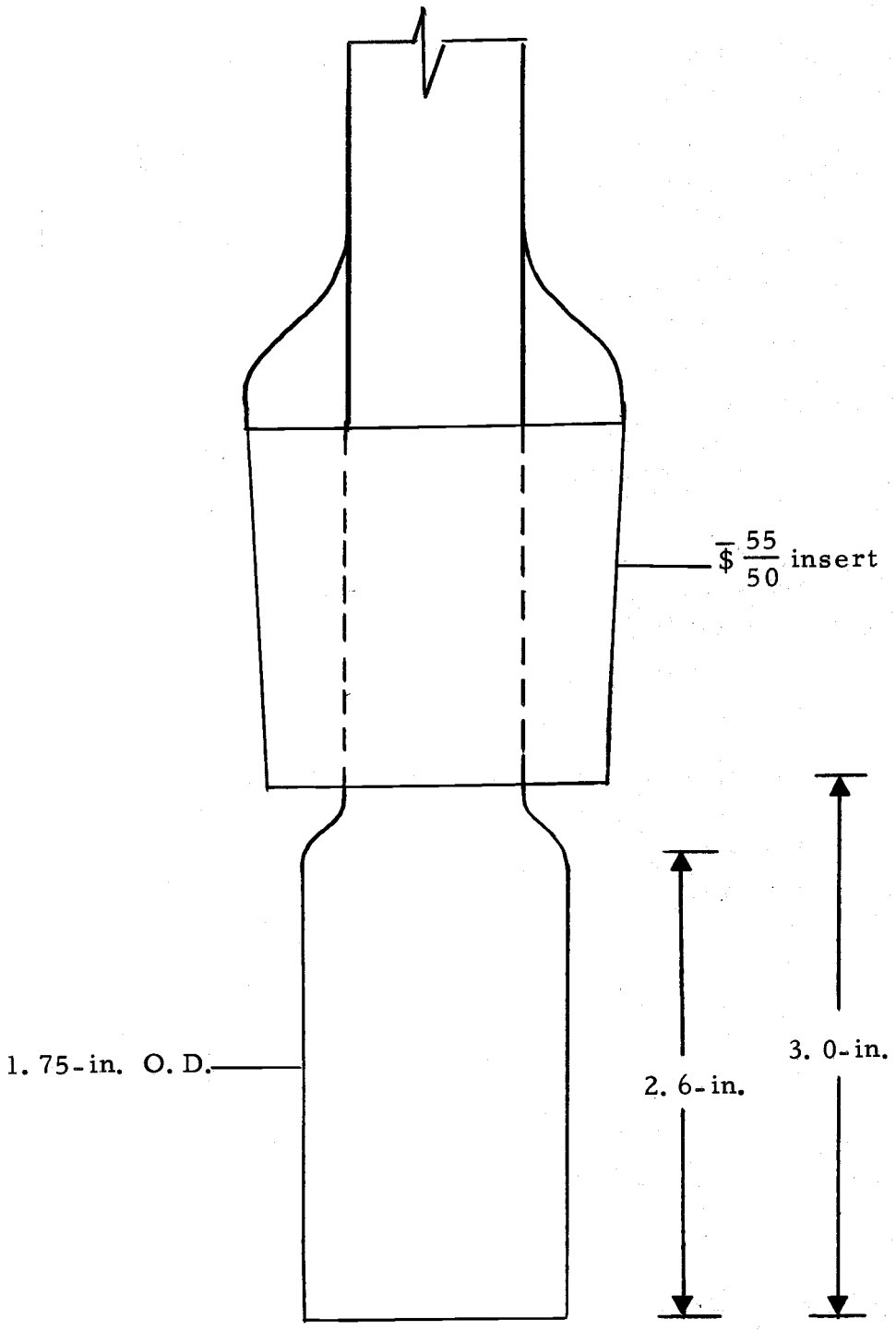

Figure 9. Bell of upper chamber.

steel beaker and the lid was fabricated from 1/2-inch thick aluminum plate. The lid and vessel were held in place by six bolts and were sealed by a neoprene rubber gasket. The boiling vessel was connected to the vapor inlet of the lower chamber by a 2.54 cm inside diameter, neoprene rubber tube which was reinforced by cloth fibers.

The power to the boiling vessel was provided by two MT-120 immersion heaters. The heaters were threaded into the reinforced bottom of the stainless steel beaker and the threads were sealed with teflon tape. The heaters were connected in series and were controlled by a 230 volt, 28 amp powerstat.

The vapor was condensed by two Friedrichs condensers, made of pyrex brand glass, which were arranged in parallel. The second condenser was vented to the atmosphere so that the system would operate as close to atmospheric pressure as possible. The condensers were cooled by ordinary tap water which was usually below 70° F. The vent line to the atmosphere was used as a safety line in case the reflux backed up into the condensers. Any excess reflux was drained into a large graduated cylinder kept in a vented hood where explosive vapors could not collect. The graduated cylinder was used to indicate the amount of material which must be returned to the system to restore it to the original conditions.

The sample points, as shown in Figure 5 as A and B, were sealed by 1-F size, self-sealing serum caps. The samples were

withdrawn from the system with a Hamilton, gas tight, teflon-gasketed, 2.5 milliliter syringe which was fitted with a number 22 needle. The sample size was less than 0.2 gm. This method allowed a sample to be removed from a well-mixed, moving liquid stream. Benzene caused the serum caps to swell, but this turned out to be advantageous since the swelling sealed the serum cap more tightly into the system. The swelling did not impair the self-sealing qualities of the rubber.

The mass flow rates of the reflux and the liquid-return to the boiling vessel were measured using tri-flat variable area flowmeters manufactured by the Fischer and Porter Company. One rotameter was 1/4-inch I.D. with 20 scale units and a constant density glass float. It had a maximum capacity of 203 cm^3 of water per minute at room conditions. The second rotameter was a 1/8-inch I.D. with 25 scale units; depending on the flow rate, a stainless steel float or a tantalum float was used. The stainless steel float had a maximum capacity of 107 cm^3 of water per minute, and the tantalum had a maximum of 171.5 cm^3 of water per minute at room conditions.

The temperature in the system was measured at eight different points, labeled TC in Figure 5. The thermocouple number and significance are as follows: TC 1, temperature of the liquid as it comes off the wetted wall; TC 2, temperature of the bath material at the inlet; TC 3, temperature of the bath material at the outlet; TC 4,

temperature of the reflux just as it approaches the knife edge; TC 5, temperature of the vapor at the bottom of the column; TC 6, temperature of the vapor at the top of the column; TC 7, temperature of the reflux at the reflux rotameter; and TC 8, temperature of the liquid at the lower rotameter. The thermocouples were made of copper-constantan wire.

The reflux was heated before it was returned to the upper liquid chamber. The heating was accomplished by a 1/2-inch by 6 feet, 288 watt, Briskeat flexible heating tape. The power was controlled by a 120 volt, 3 amp powerstat.

The vapor leaving the reflux column was heated to prevent if from condensing and returning to the upper liquid chamber. This was accomplished using a 1-inch by 6 feet, 384 watt, Briskeat flexible heating tape. The power was controlled by a 120 volt, 3 amp powerstat.

The column was surrounded by a 3-inch outside diameter tube and was connected to the system by means of a standard taper joint. A mixture of water and ethylene glycol was used as the heat transfer medium. The mixture was heated using one 688-watt and two 348-watt immersion type heaters. One of the heaters was controlled by a Fisher unitized bath control. The other heaters were controlled by 120 volt, 3 amp powerstats. The heating material was pumped by a Deming centrifugal pump equipped with a sparkless motor. The flow

rate was measured by a Fischer and Porter precision bore rotameter, type 5A-25-A.

Analyses of the liquid composition at points A and B were accomplished using a Bausch and Lomb precision refractometer of the modified Abbé type. The temperature of the refractometer prisms was maintained at a constant value of 25° C by means of a constant temperature bath. A calibration chart was prepared by measuring the index of refraction of samples of known composition.

DESCRIPTION OF SYSTEM STUDIED

The binary system of benzene-n-butanol was chosen for this investigation. This system was chosen specifically because the relative volatility was fairly high, about 4.5. Accordingly, an appreciable difference between the dew-point temperature and the bubble-point temperature for the same composition resulted. The components had an appreciable difference in refractive index which provided a convenient, accurate method of analyzing compositions. Since the hot liquid was a powerful solvent, the joints were made of precision ground glass joints, thus eliminating silicone stopcock grease which would dissolve in the hot liquid. The tightness of the joints was required due to the toxicity of the vapors.

The vapor-liquid equilibrium data at atmospheric pressure were obtained from the results of Yerazunis, Plowright and Smola (35). The data are presented in Appendix B and are shown for the entire composition range in Figure 30. The data had been smoothed and tested for thermodynamic consistancy by the composition-resolution method of testing vapor-liquid equilibrium data of Van Ness (32) and had been found to be consistent. The vapor-liquid equilibrium data were necessary to determine the number of transfer units in the column.

The benzene was of U.S.P. grade and was supplied by the Van

Waters and Rogers Scientific Supply Company. The n-butanol was of reagent grade and was manufactured by the Baker and Adamson Chemical Company. The refractive index of the n-butanol was found to be 1.39762 compared to 1.39931 for the true value at 25°C.

OPERATING PROCEDURE

Before any data were taken, the equipment was run for several days to acquaint the author with the running problems and to clean the system of any impurities. The flushing of the system was necessary after it was found that the hot benzene-n-butanol mixture would dissolve silicone stopcock grease. The joints were cleaned and the silicone grease was not applied again.

Power to the reboiler heaters was adjusted until the desired vapor mass flow rate through the column was obtained. The liquid level in the lower chamber was adjusted to the bottom of the wetted-wall column and held there throughout the entire run. The next step was to adjust the power to the reflux heating tape until the temperature of the reflux liquid in the upper chamber was within 2° C of the bubble-point of the mixture.

The temperature of the fluid in the temperature control bath was heated to the desired temperature. This fluid was circulated through the outside tube for the entire run.

The entire system was allowed to run for about one-half hour before the first sample was taken. A small sample of the liquid stream was then taken about every five minutes until three consecutive samples agreed to within 0.02 refractometer scale units or within 0.04 mole percent and to where there was no trend shown by the three

consecutive runs. The samples were about 0. 2 grams in size, which constituted less than 0. 2 mole percent of the entire reflux section. The composition of the mixture was determined by measuring the refractive index of the mixture with a Bausch and Lomb precision refractometer of the modified Abbé type. The prisms had been held at 25°C by a constant temperature bath. After the column's operations were determined to be at steady-state, the temperature at each of the thermocouple locations was measured. The temperature at the potentiometer, made by the Leeds and Northrup Company, was measured by a mercury thermometer which was graduated in 0. 1°C increments. The reference junction was set by means of a thermocouple set beside the thermometer.

PRESENTATION AND DISCUSSION OF RESULTS

The value of N_{OG} was measured over as large a range as possible. The results are presented in Figure 10. The concentration dependence below 23 mole percent benzene was not investigated because the surface tension effects at lower concentrations caused the liquid to channel and not wet the wall completely. The phenomenon of channeling as a function of concentration and temperature changes has been investigated elsewhere (8, 36). The concentration dependence of N_{OG} was not investigated above a vapor inlet composition of 83 mole percent benzene where the amount of separation was too small to be accurate. The values of N_{OG} were calculated using Simpson's three-point integration formula. The accuracy of this method was checked in the composition range where the vapor liquid line was a straight line. In this region, Equation (1) could be integrated analytically to obtain the experimental value of N_{OG}. The results for the two methods were identical. The values of N_{OG}, shown in Figure 10 were plotted versus $\frac{1}{2}(y_{AO}+y_{AT})$ so that comparisons could be made with the results of previous investigations (11, 17, 22, 27, 30). The results are similar to the previous investigations showing a variation of about 30 percent over the average vapor composition range of 38 to 85 mole percent benzene.

The number of transfer units based on experimental conditions

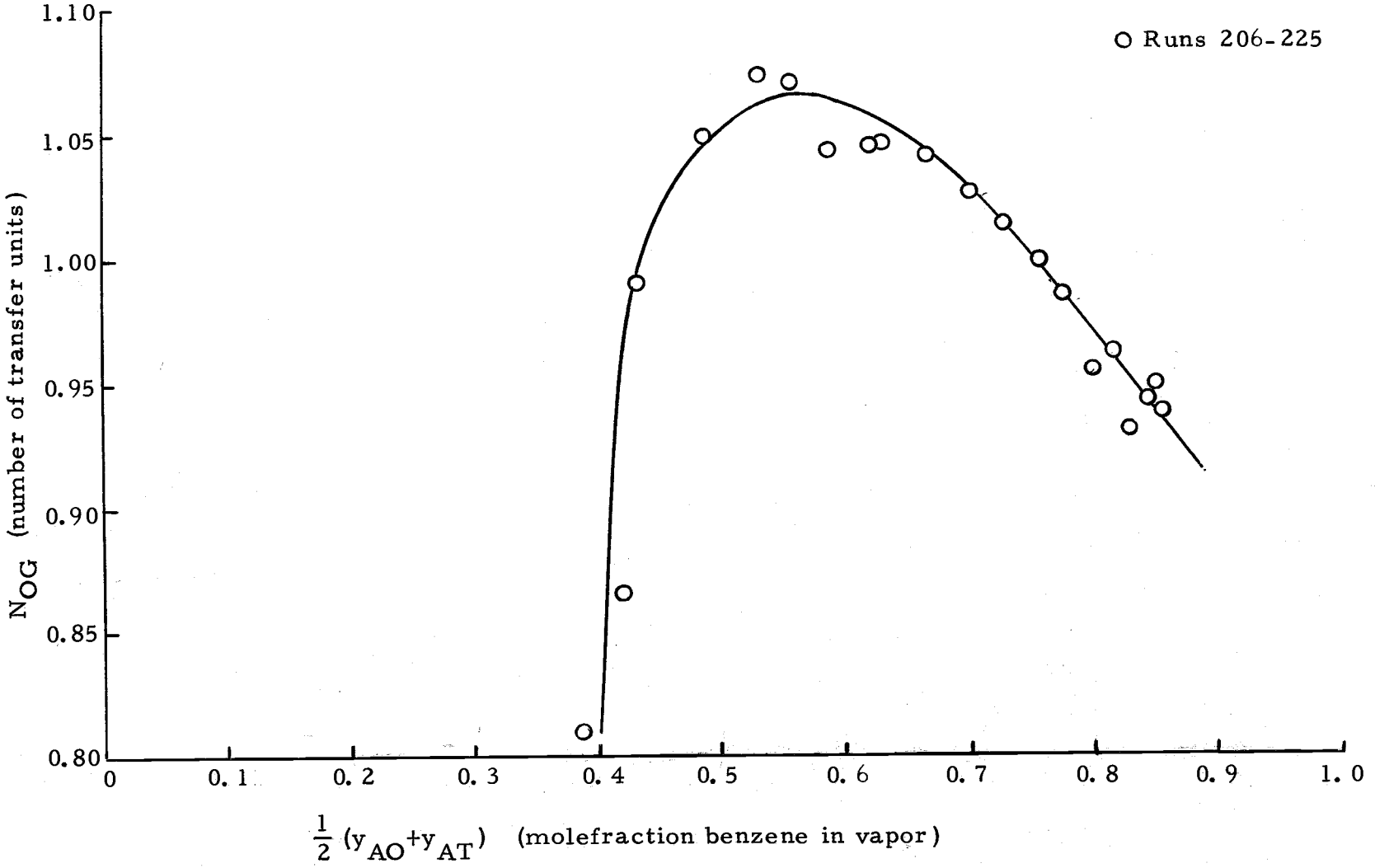

Figure 10. Number of transfer units versus average composition for benzene-n-butanol.

and analogy equations were calculated in the same manner as Hutchison and Lusis (17). The height of a transfer unit based on the overall driving force $(y_A^* - y_A)$ is a function of the liquid film transfer height H_{TL}, the vapor film transfer height H_{TG}, the slope of the equilibrium line m and the ratio of the vapor flow rate to the liquid flow rate. For total reflux the ratio of vapor flow rate to the liquid flow rate is one. The relationship between H_{OG}, H_{TL}, H_{TG} and m then becomes

$$H_{OG} = H_{TG} + mH_{TL} \tag{38}$$

The vapor film transfer height H_{TG} was calculated using the equation of Gilliland and Sherwood (12).

$$H_{TG} = 10.9 D_t (Re_G)^{0.17} (Sc_G)^{0.56} \tag{39}$$

The viscosity, mass diffusivity and density of the vapor were predicted using the equations shown in Appendix C. The liquid film transfer height was calculated using the correlation from the gas absorption experiments made by Hakita, Nakanishi and Kataoka (14).

$$H_{TL} = 2.35 \left(\frac{M_B}{M}\right) (Re_L)^{1.0} (Sc_L)^{1/2} \left(\frac{\rho^2 g}{\mu^2}\right)_L^{-1/3} \tag{40}$$

M_B is the molecular weight of the n-butanol and M is the mean

molecular weight of the mixture. The liquid mass diffusivity was calculated using the Wilke and Chang method (34).

$$\frac{D_L \mu}{T} = 7.4 \times 10^{-8} \frac{(XM_A)^{0.5}}{(V_O)^{0.6}} \tag{41}$$

For benzene X was given as 1.0 M_A was the benzene molecular weight and V_O was the atomic volume of benzene at its normal boiling point calculated from the data of LeBas (21). Since this equation is derived for low concentrations, it was necessary to extend it to higher concentrations as diffusion data were not available for higher concentrations. The liquid viscosity of the liquid mixture was predicted from the pure component viscosities using the Kendall-Monroe (18) equation.

$$\mu_m^{1/3} = x_A \mu_A^{1/3} + x_B \mu_B^{1/3} \tag{42}$$

The value of x_A is the mole fraction of A in the liquid phase.

The value of m was calculated by taking the slope of the vapor-liquid equilibrium curve based on the data of Yerazunis, Plowright and Smola (35).

The values of H_{TG} and H_{TL} varied only slightly over the entire concentration range, and thus the major variation shown by H_{OG} was due to the large variation in m. The value of H_{TL} was about 14 percent of H_{TG}, which agrees very well with Hutchison and

Lusis (17). The calculated value of H_{OG} was used to calculate N_{OG} by Equation (43).

$$N_{OG} = z/H_{OG} \tag{43}$$

The known height of the column is z.

The calculated results for N_{OG} are shown in Figure 11 which also shows the experimental curve. The two curves shown in Figure 11 compare with each other in the same manner as does the experimental and theoretical curves of Hutchison and Lusis (17). The calculated results compare within 10 percent in the intermediate composition range, but it does not predict the strong variation over the entire composition range. This agrees also with the investigations of Sawistowski and Smith (30).

Because N_{OG} varied considerably with composition, it was desirable to investigate the composition dependence of N'_{OG}, the transfer unit which includes thermal effects. As a first step in evaluating N'_{OG}, each of the terms in $\phi(y_A, y_{Ai})$ will be discussed.

The convective heat transfer term

$$\frac{2y_{Ai}h_V(T_G - T_i)}{(r-\delta)\lambda_{mi}K'_G a} \tag{44}$$

may be estimated by using the Chilton-Colburn analogy (5) for determining the value of h_V. It was necessary to make assumptions

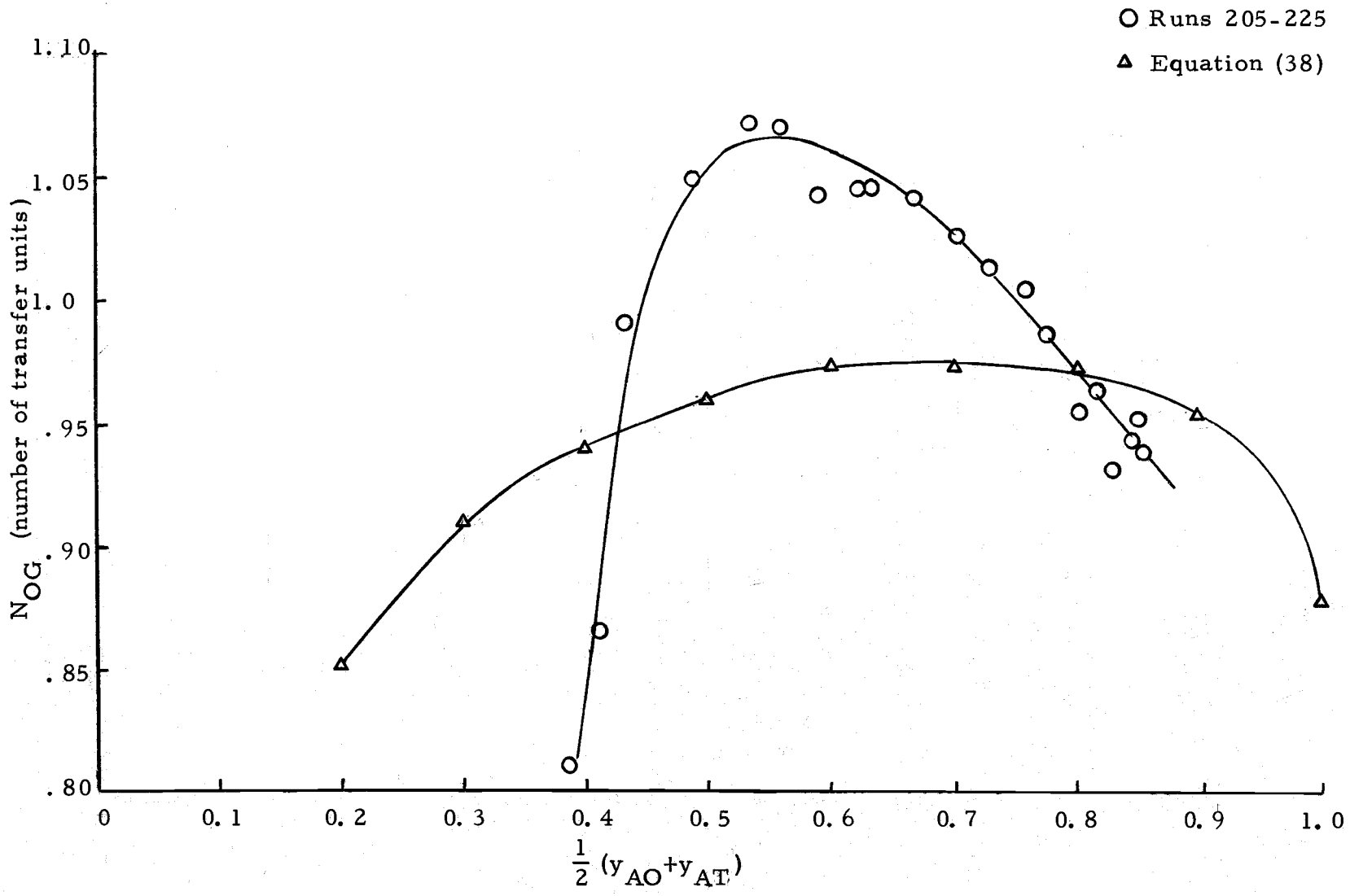

Figure 11. Comparison of experimental results with gas absorption predictions.

concerning the interfacial temperature and composition. The value of T_i was initially assumed to be the bulk liquid saturation temperature, T_L, and y_{Ai} was assumed to be y_A^*, the vapor phase composition in equilibrium with the bulk liquid composition, x_A. The value of λ_{mi} was calculated at the saturated liquid temperature and at the assumed interfacial composition, y_A^*. The molecular diffusivity in the vapor phase was calculated using the Hirschfelder, Bird and Spotz equation (15). The thermal conductivity was estimated using the Euchen equation (10), and the viscosity of the vapor was estimated using the Chapman-Enskog equation (2). These equations and a discussion of them can be found in Appendix C. The thickness of the liquid film, δ, was estimated using the Nusselt equation for a flat plate (24).

$$\delta = 0.909\ (Re_L)^{1/3} \left(\frac{g\rho^2}{\mu^2}\right)_L^{-1/3} \qquad (45)$$

For pure benzene, δ was 0.0148 cm and for pure n-butanol, δ was 0.0187 cm. This was less than 2 percent of the total diameter. The value of a mixture would be some intermediate value between 0.0148 cm and 0.0187 cm. The variation of the heat transfer term with composition is shown in Figure 12. The magnitude of the heat term relative to the magnitude of $(y_A^* - y_A)$ for benzene-n-butanol is shown in Figures 13 and 14. It can be seen that the magnitude of the

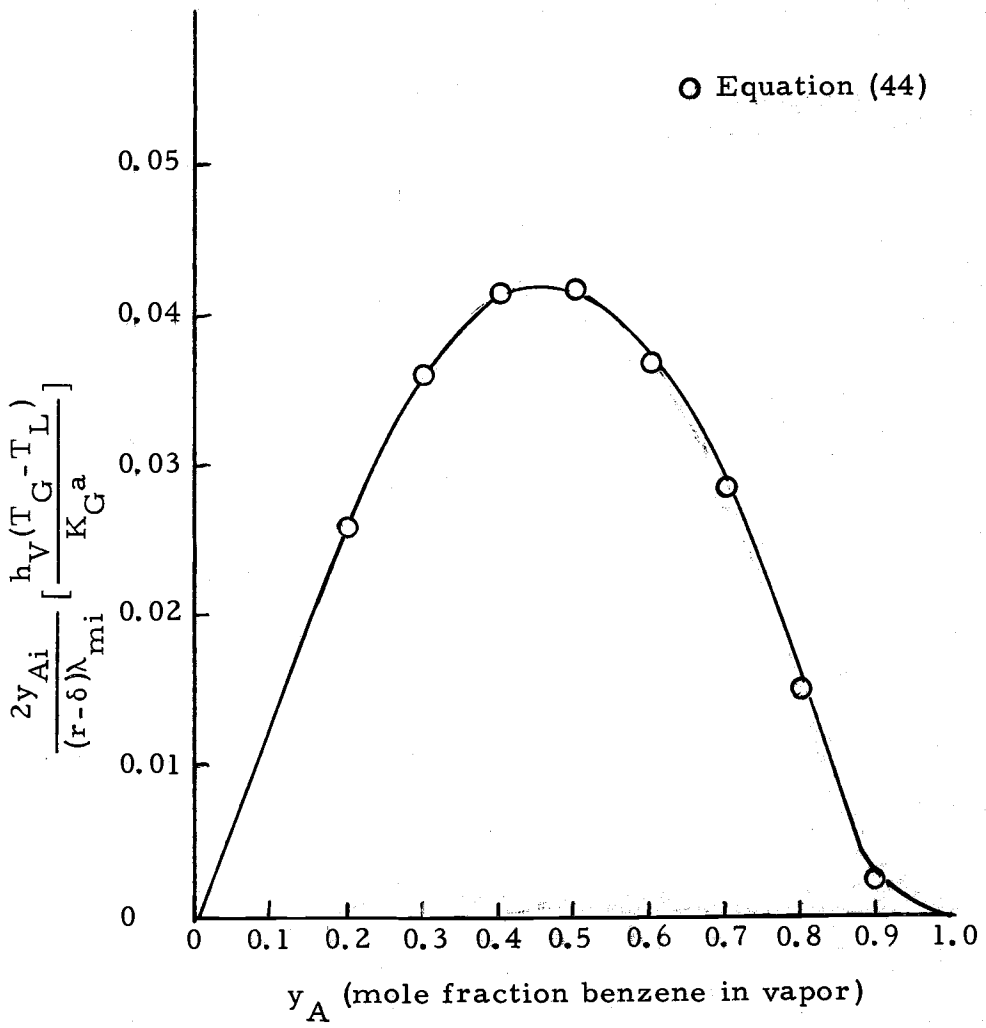

Figure 12. Heat transfer contribution to the driving force.

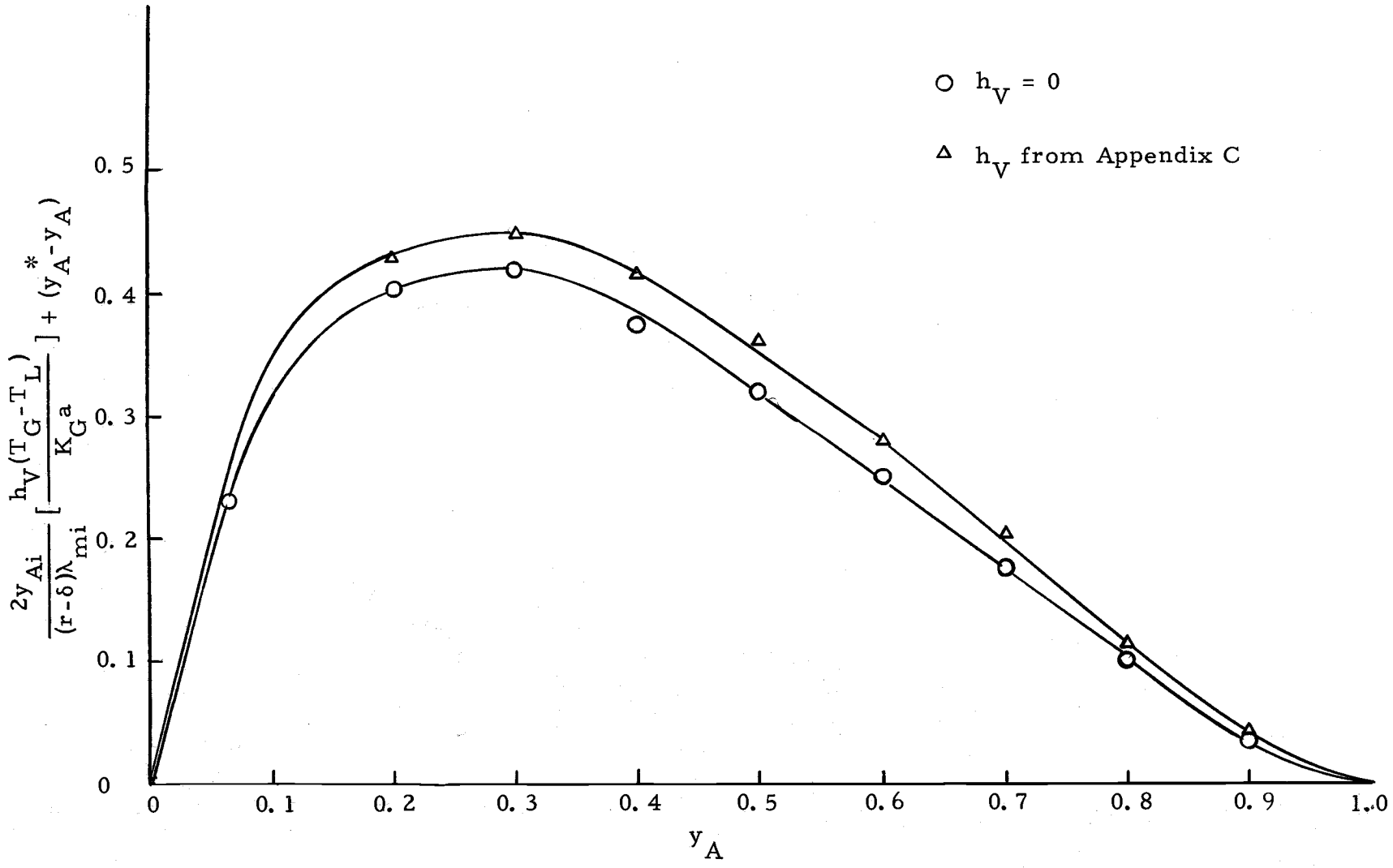

Figure 13. Concentration driving force with temperature driving force.

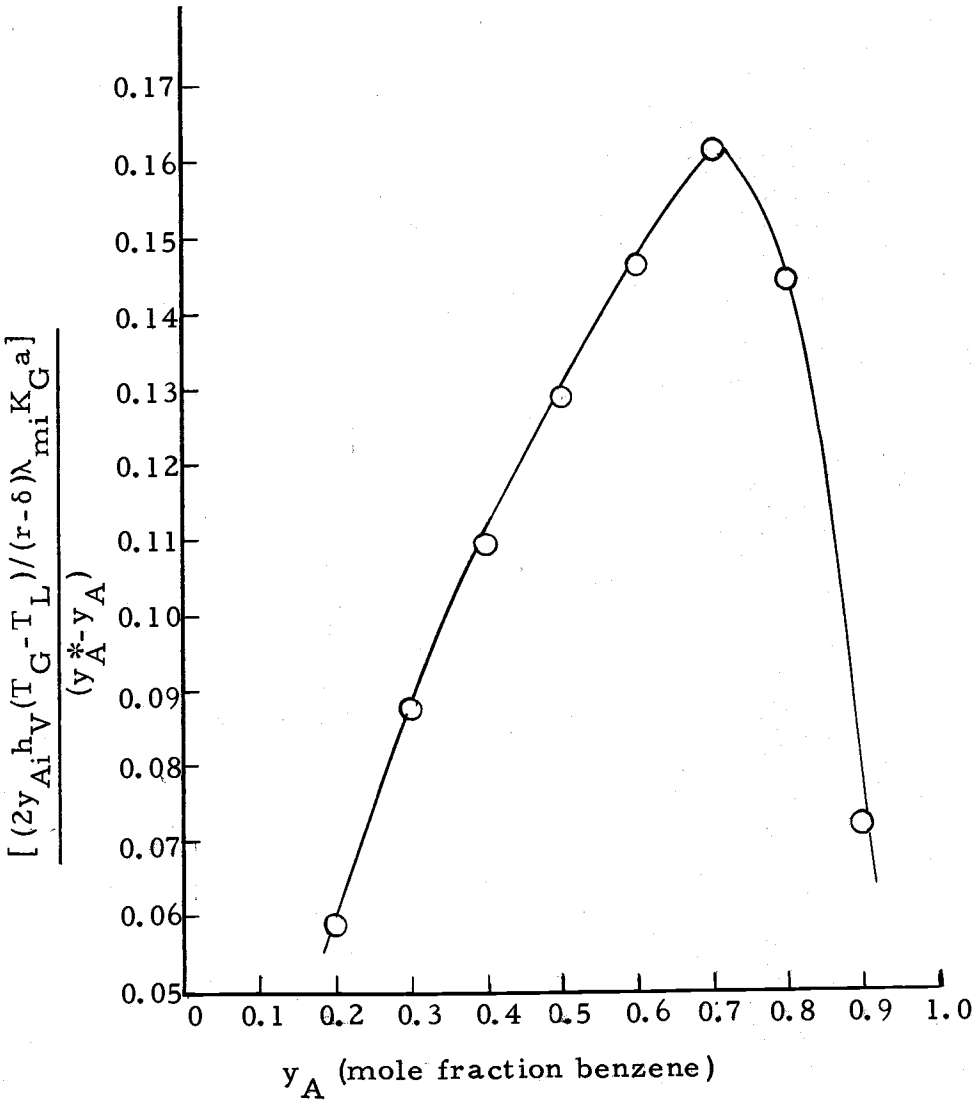

Figure 14. Ratio of thermal to concentration driving force.

thermal term has a maximum near the vapor composition $y_A = 0.47$. However, the magnitude of the heat transfer term relative to the magnitude of $(y_A^*-y_A)$ is a maximum near the vapor composition $y_A = 0.70$.

To check the assumption on the interfacial temperature and composition, an estimate was made of the true interfacial conditions, using the results for H_{TG} and H_{TL} obtained earlier in this discussion. It was found that the largest error was in the benzene composition range below 30 mole percent benzene, about 30 percent deviation. Above 30 mole percent, where all the experimental data was taken, the deviation became small very fast, about seven percent for y_A equal to 0.50 and four percent for y_A equal to 0.80. It should be noted that these deviations are only estimates since they are based on data which predicts a curve ten percent below what was actually observed.

Table 1. Comparison of assumed and estimated interfacial conditions.

y_A	y_A^*	y_{Ai}	T_L	T_i
0.2	0.620	0.553	97.7	101.2
0.5	0.820	0.806	85.8	87.1
0.8	0.900	0.899	81.5	81.7

Since the heat transfer term will always be positive, and its magnitude is important when compared to $(y_A^*-y_A)$, this term would cause an increase in the column separation, $(y_{AT}-y_{AO})$.

The value of

$$-\frac{1}{K_G a}\frac{1}{\lambda_{Ai}}\frac{d}{dz}(GC_{PL}(T-T_{ref})) \tag{46}$$

can not be calculated from experimental data as a point function since the temperature and composition are not known as function of the column height. However, for an estimate of the relative magnitude, the value at average conditions can be calculated. The change in sensible heat is calculated by integrating the heat capacity equation which is assumed to vary linearly over the height z.

$$\frac{1}{K_G a}\frac{1}{\lambda_{Ai}}\frac{d}{dz}(GC_{PL}(T-T_{ref})) \doteq (\frac{G}{K_G a})\frac{1}{G\lambda_{Ai}}\frac{\int_{T_O}^{T_T} GC_{PL}\,dT}{z}$$

$$\doteq \frac{z}{N_{OG}}\frac{1}{G\lambda_{Ai}}\frac{\int_{T_O}^{T_T} GC_{PL}\,dT}{z}$$

$$\doteq \frac{1}{N_{OG}G\lambda_{Ai}}\int_{T_O}^{T_T} GC_{PL}\,dT \tag{47}$$

The value of the approximation as a function of the average composition is shown in Figure 15. The graph shows a larger negative value at the intermediate composition range, that is between $\frac{1}{2}(y_{AO}+y_{AT})$ equal to 0.3 and 0.5, but decreases rapidly as higher concentrations

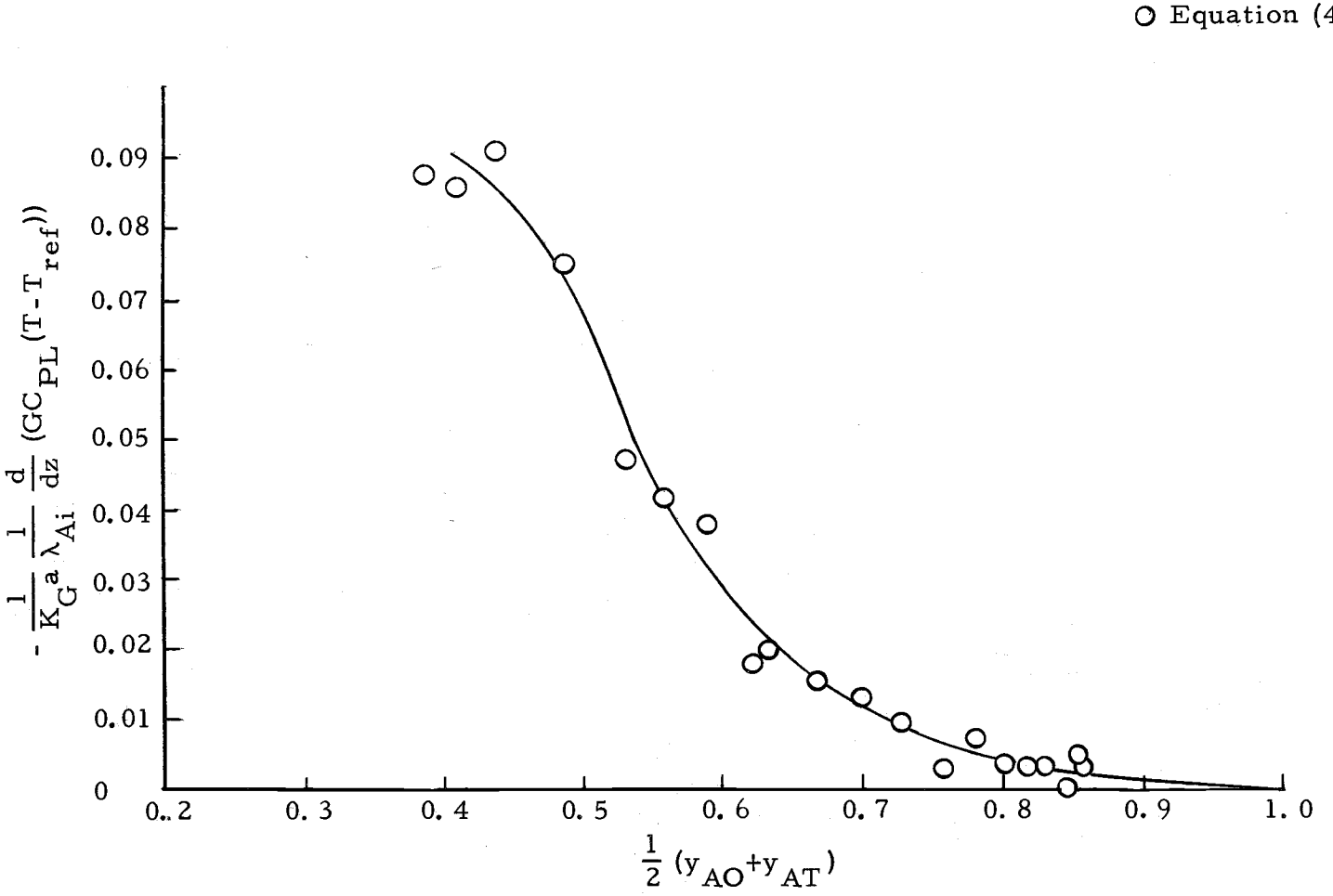

Figure 15. Reduction in driving force due to sensible heat requirements.

are approached. Since this term is negative, it will tend to decrease the possible separation.

The next term to be considered is the term which deals with the rate of change of the difference between the liquid and vapor specific enthalpies with position in the column. Since the composition in the column is not known as a function of column height, it is necessary for the sake of qualitative discussion to assume a linear dependence.

$$\left(\frac{G}{K_G a}\right)\frac{y_A}{(H_G-H_L)}\frac{d(H_G-H_L)}{dz} \doteq \frac{z y_A\left[(H_G-H_L)_T-(H_G-H_L)_O\right]}{N_{OG}\left\{\frac{1}{2}\left[(H_G+H_L)_O+(H_G+H_L)_T\right]\right\}z}$$

$$\doteq \frac{2y_A\left[(H_G-H_L)_T-(H_G-H_L)_O\right]}{N_{OG}\left[(H_G-H_L)_T+(H_G-H_L)_O\right]} \qquad (48)$$

The value of (H_G-H_L) is approximated by assuming the liquid interfacial temperature to be equal to the bulk liquid temperature.

$$(H_G-H_L) \doteq \lambda_{mi} + \int_{T_i}^{T_G} C_{PGm}\,dT \qquad (49)$$

The variation of (H_G-H_L) with composition is shown in Figure 16. Experimental data are used for the inlet and outlet conditions in Equation (48). The results, shown in Figure 17, are negative relative to $(y_A^*-y_A)$ and therefore will reduce the efficiency and the separation of the column.

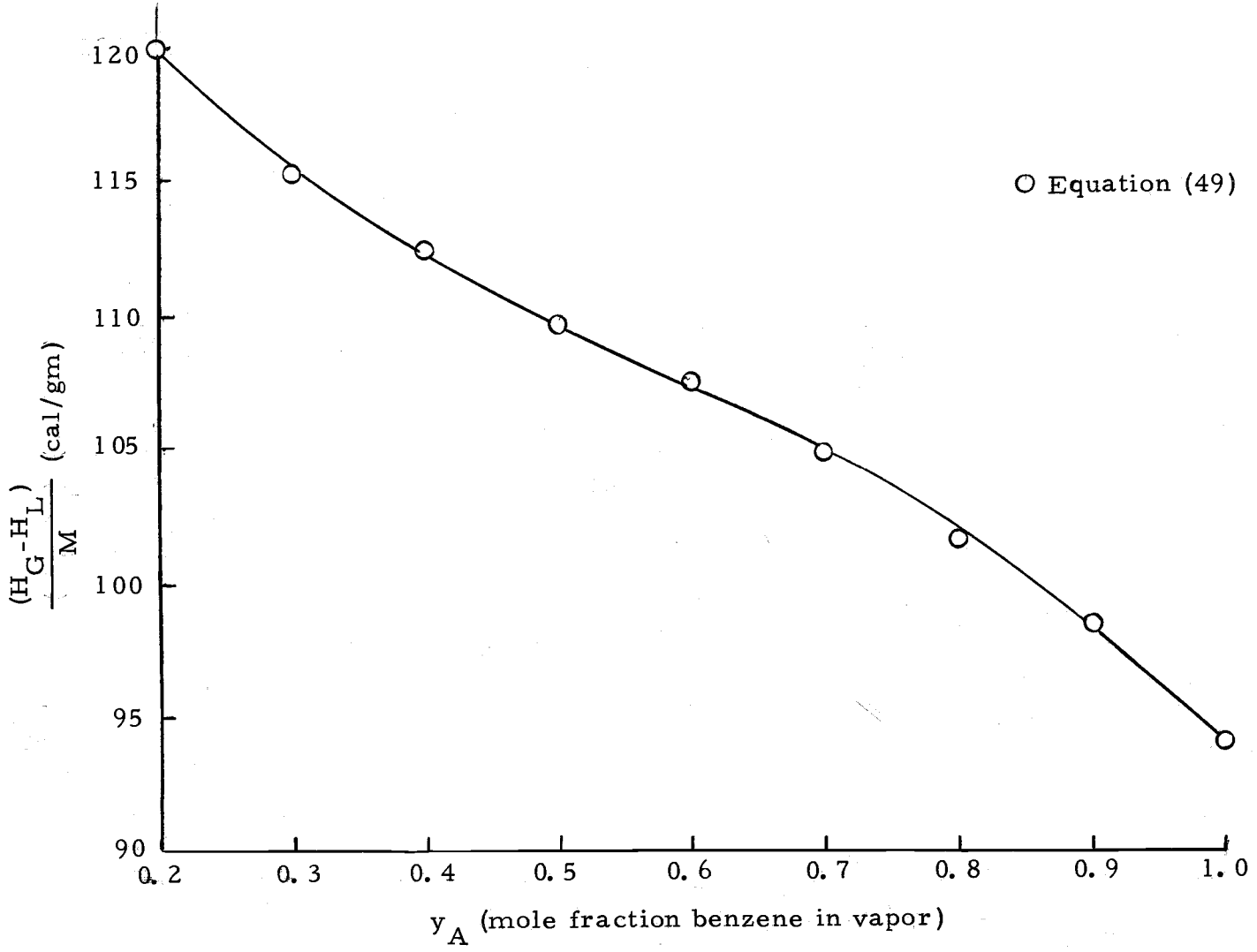

Figure 16. Approximate enthalpy difference between the vapor and the liquid.

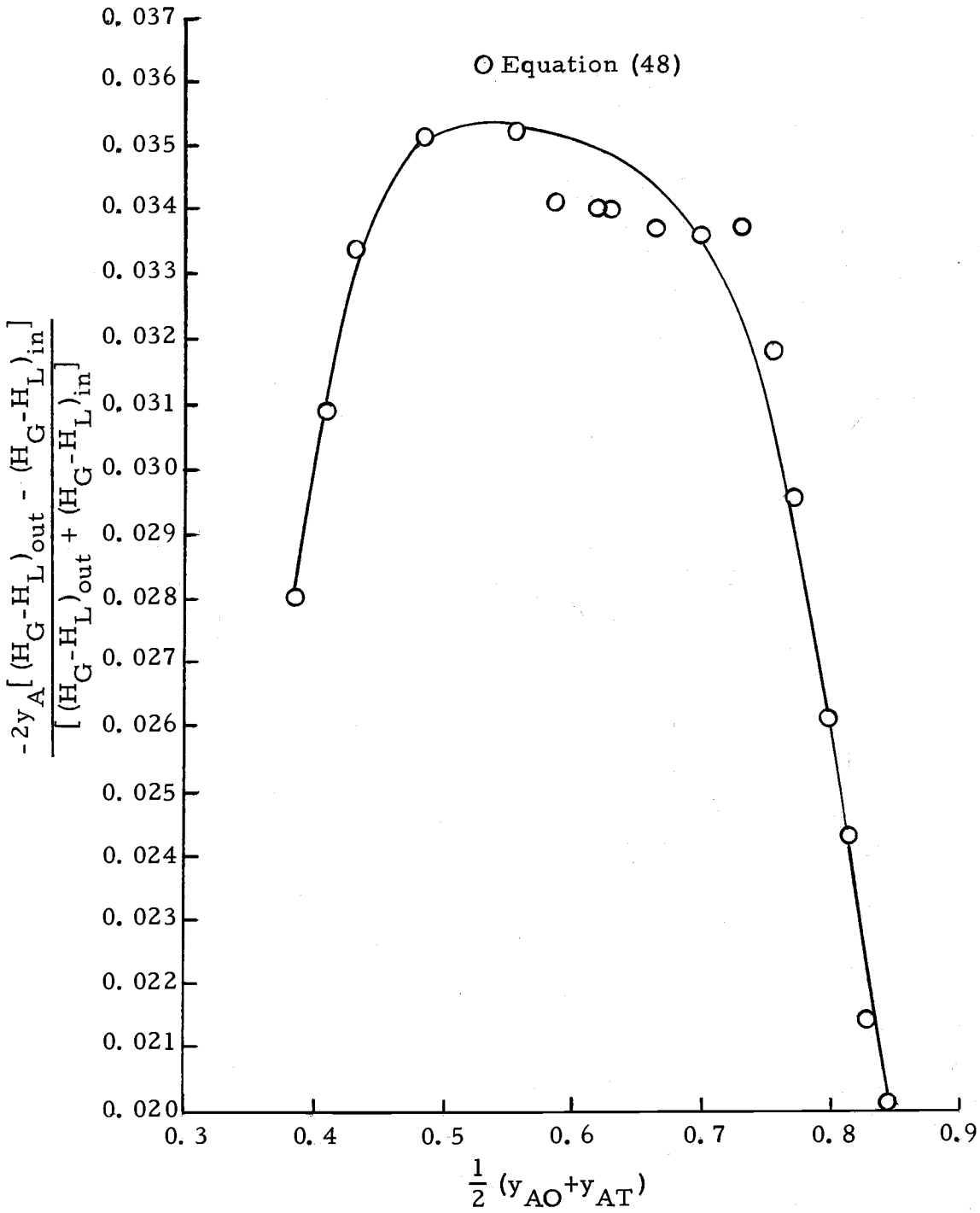

Figure 17. Enthalpy correction for the driving force.

The contribution of the heat of mixing term can be approximated from the present experimental data and from heat of mixing data in the literature. Heat of mixing data for benzene-n-butanol are available for 25° C, 35° C and 45° C (23). If this set of data is used as the basis for the straight line approximation shown in Figure 18, the higher temperature values can be estimated. The same linear approximation is made as before.

$$-\left(\frac{1}{K'_G a}\right)\left(\frac{1}{\lambda_{Ai}}\right)\frac{d}{dz}\left(G\Delta H_m\right) \doteq -\left(\frac{G}{K'_G a}\right)\left(\frac{1}{G\lambda_{Ai}}\right)\frac{G\left[\left(\Delta H_m\right)_T-\left(\Delta H_m\right)_O\right]}{z}$$

$$\doteq -\frac{\left[\left(\Delta H_m\right)_T-\left(\Delta H_m\right)_O\right]}{N_{OG}\lambda_{Ai}} \qquad (50)$$

The heat of mixing terms, ΔH_m, were calculated at the temperature and concentration at the inlet and outlet conditions. To calculate the contribution as a function of the height in the column, it would be necessary to know the partial molal heat of mixing as well as the concentration as a function of the position in the column.

The contribution of the heat of mixing will be a positive quantity for the benzene-n-butanol system. The relative magnitude for three runs are given in Table 2.

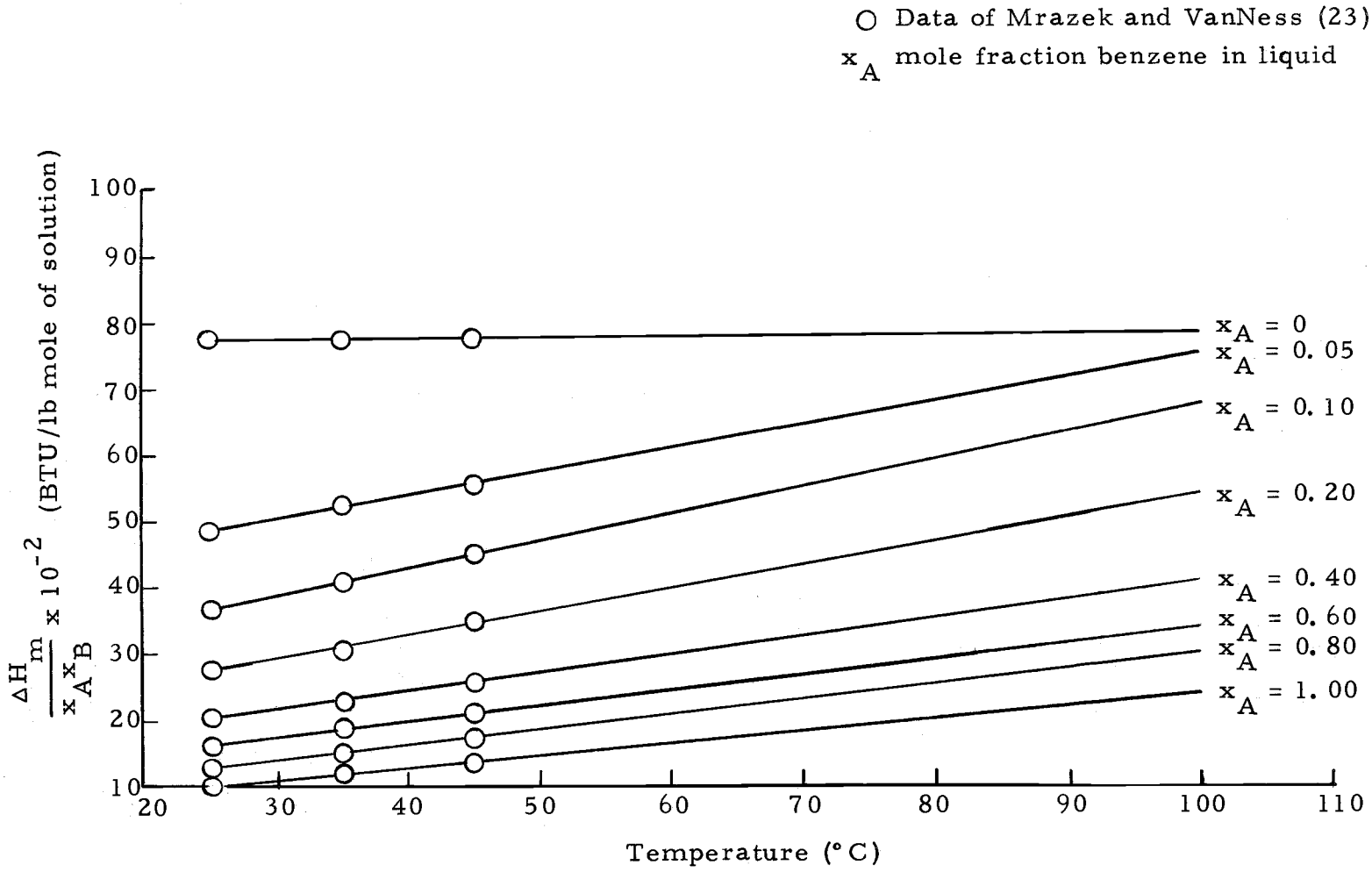

Figure 18. Heat of mixing as a function of temperature.

Table 2. Heat of mixing contribution for three runs.

Run number	$\frac{1}{2}[y_{AO}+y_{AT}]$	$-\frac{[(\Delta H_m)_T-(\Delta H_m)_O]}{N_{OG}\lambda_{Ai}}$
206	0.3860	0.0090
211	0.5325	0.0143
225	0.8556	0.0081

The magnitude of $(N'_B-N_B)\frac{\lambda_{Bi}}{\lambda_{Ai}}$ cannot be calculated without very accurate mass flow data. The mass flow data taken in the experimental runs were accurate only within a few percent, which, because differences were taken, made the errors quite large. The ratio of the mass of benzene vaporized to the mass of n-butanol condensed is shown in Figure 19. It should be noted that the maximum ratio is between 0.6 and 0.7 mole fraction benzene. In the intermediate concentration range the vaporization of benzene is larger than the condensation of n-butanol even though this is the region where the negative thermal effects have their greatest absolute magnitude. The ratio decreases rapidly as higher concentrations are approached indicating the negative effects are controlling. This would indicate that N_{OG} should decrease sharply, which agrees with the experimental data.

As was stated in the discussion of the present theory, it was decided that $[\phi(y_A, y_{Ai})+\phi'(y_A, y_{Ai}, T_b)]$ could be investigated by varying the $\phi'(y_A, y_{Ai}, T_b)$ values, realizing the total

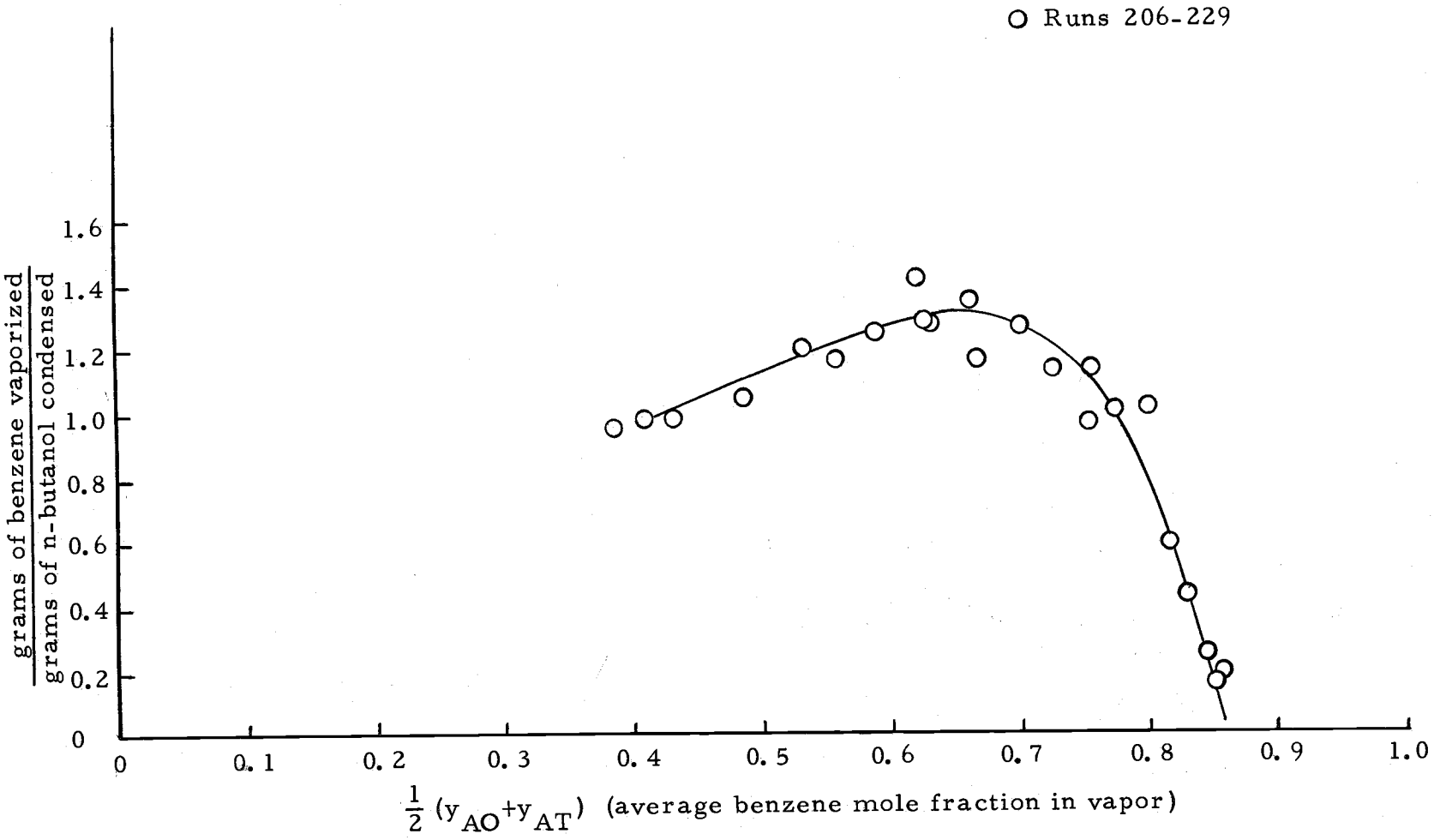

Figure 19. Ratio of benzene vaporized to n-butanol condensed.

$[\phi(y_A, y_{Ai}) + \phi'(y_A, y_{Ai}\ T_b)]$ would change. This would be accomplished by varying T_b, the heat transfer fluid temperature, which would cause heat energy to be added to or withdrawn from the system. The fluid at the desired temperature was circulated through the annular space surrounding the wetted-wall column. The values of the Chilton-Colburn N_{OG} were then calculated from the data obtained to see how N_{OG} varied as a function of the average temperature difference between the heat transfer fluid and the liquid on the inside of the wetted-wall column. The results are shown for three average compositions, $\frac{1}{2}(y_{AO}+y_{AT})$, in Figures 20, 21 and 22.

To estimate the influence of $\phi'(y_A, y_{Ai}, T_b)$ on N'_{OG}, an assumption must be made which will put $\phi'(y_A, y_{Ai}, T_b)$ in a form which can be easily handled. In the definition of $\phi'(y_A, y_{Ai}, T_b)$, given in Equation (28), there is a term $\{y_{Ai}/\lambda_{mi} - y_A/(H_G-H_L)\}$. Since (H_G-H_L) is slightly larger than λ_{mi} and y_{Ai} is slightly less than y_A^* in the concentration range greater than 50 mole percent benzene, then $\{y_{Ai}/\lambda_{mi} - y_A/(H_G-H_L)\}$ is very nearly equal to $(y_A^*-y_A)/\lambda_{mi}$. When this is true, Equation (28) is approximately equal to Equation (52).

$$\phi'(y_A, y_{Ai}, T_b) = \frac{1}{K'_G a}\left[\frac{2rh_b(T_b-T_L)}{(r-\delta)^2}\left\{\frac{y_{Ai}}{\lambda_{mi}} - \frac{y_A}{(H_G-H_L)}\right\}\right] \qquad (51)$$

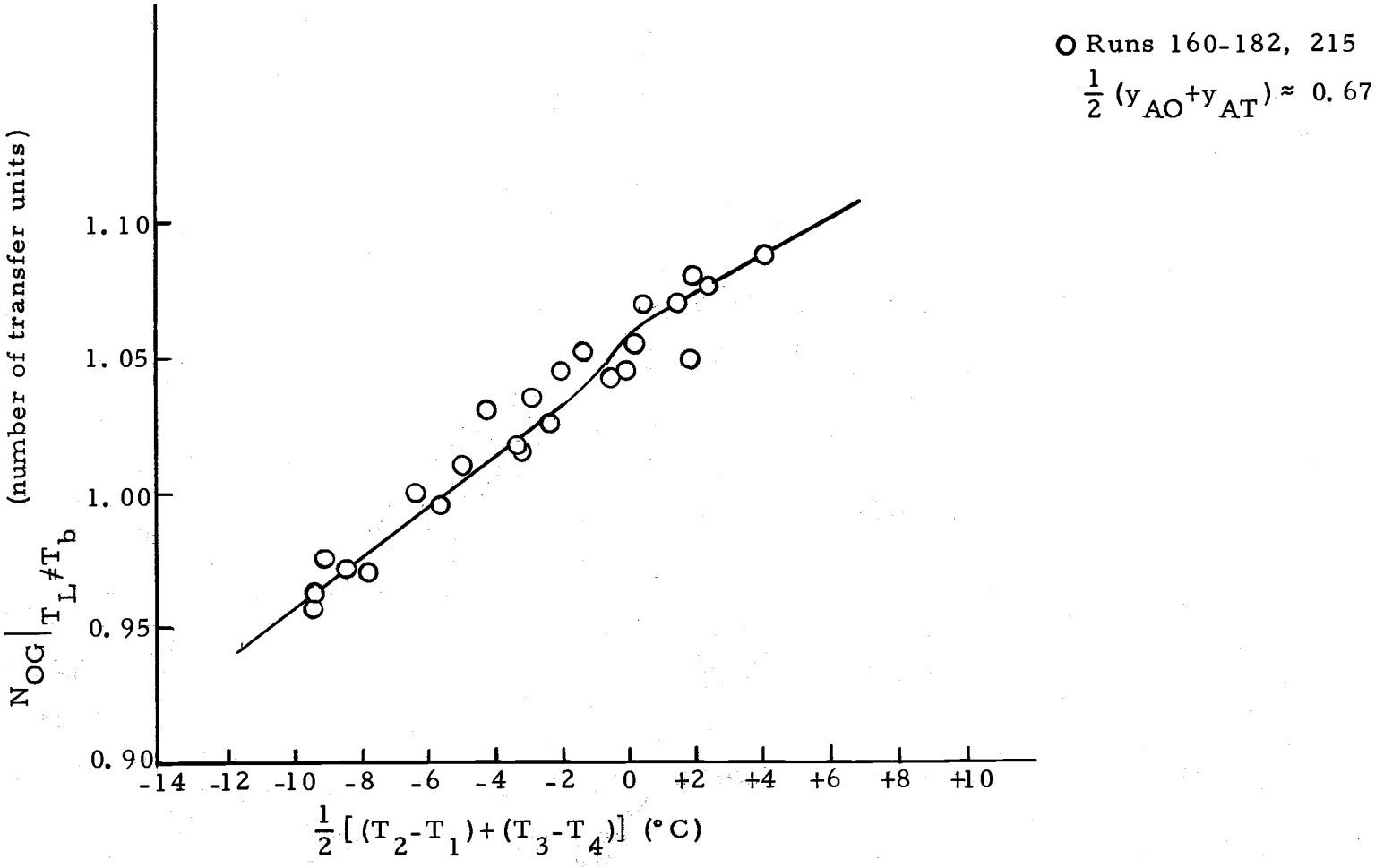

Figure 20. Number of transfer units versus the average temperature difference between the heat transfer fluid and the reflux liquid.

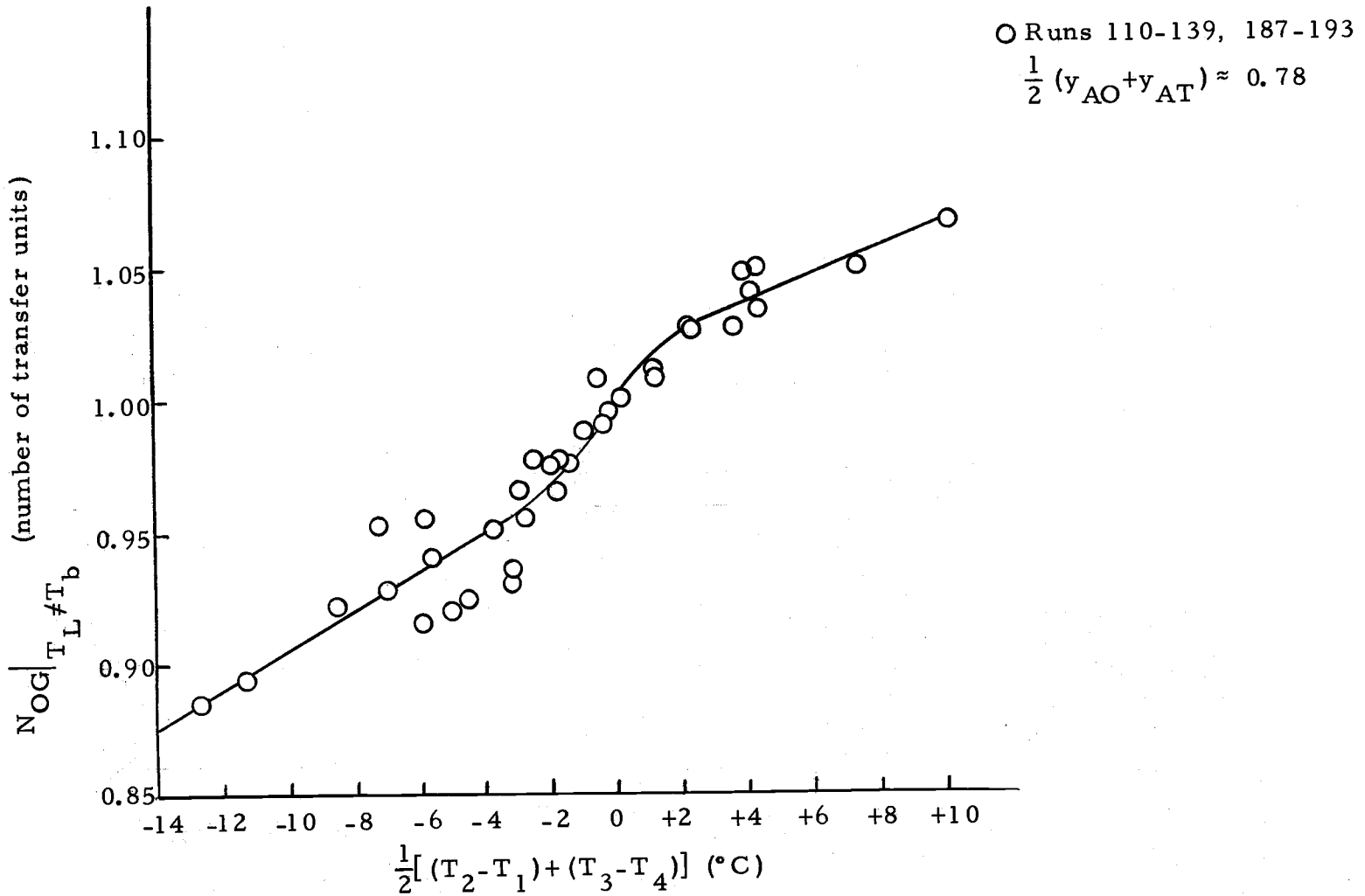

Figure 21. Number of transfer units versus the average temperature difference between the heat transfer fluid and the reflux liquid.

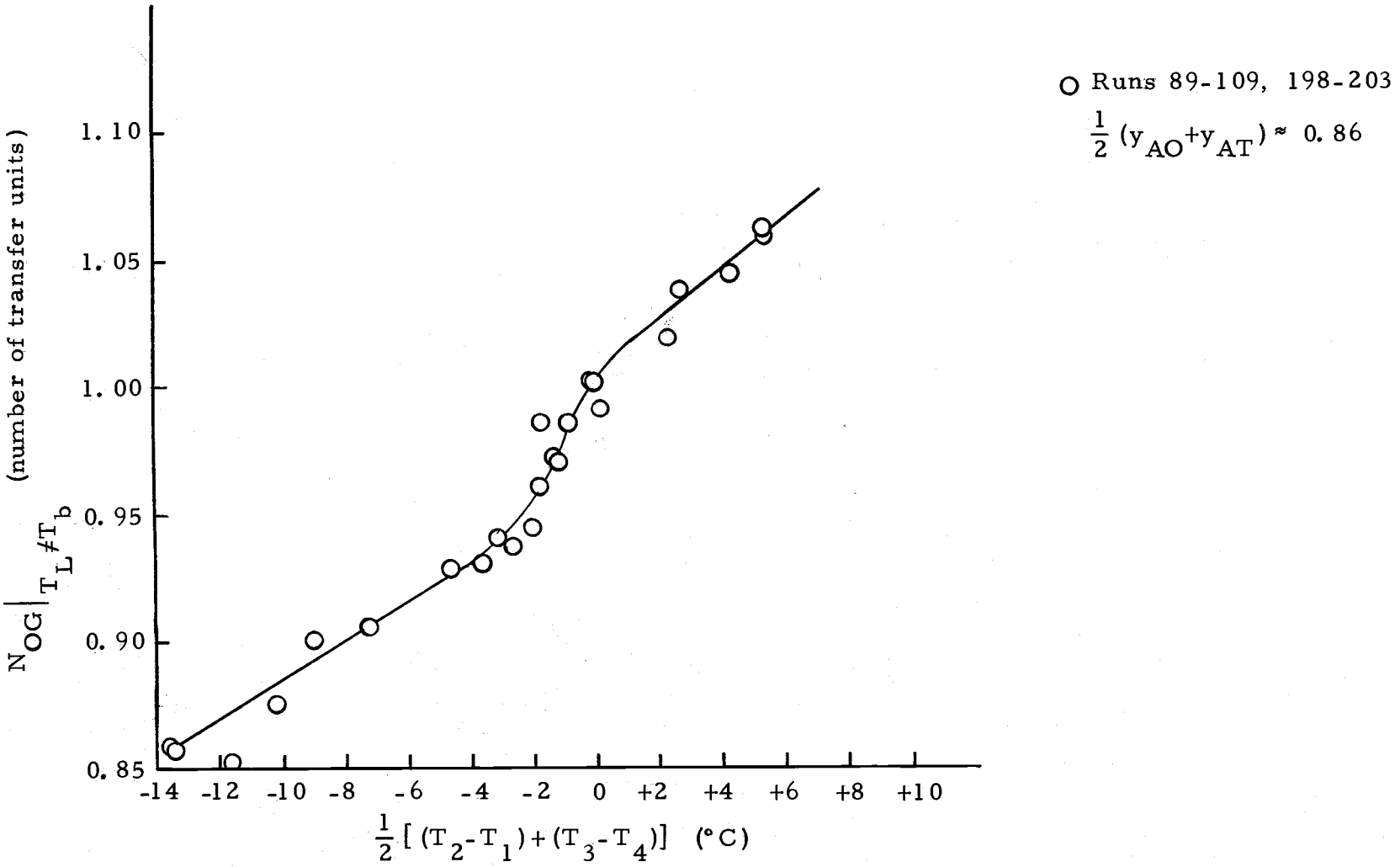

Figure 22. Number of transfer units versus the average temperature difference between the heat transfer fluid and the reflux liquid.

$$\phi'(y_A, y_{Ai}, T_b) \doteq \left\{\frac{2rh_b(T_b-T_L)}{K'_G a \lambda_{mi}(r-\delta)^2}\right\} (y_A^*-y_A) \tag{52}$$

For convenience the term in the brackets will be defined as ξ.

$$\xi = \left\{\frac{2rh_b(T_b-T_L)}{K'_G a \lambda_{mi}(r-\delta)^2}\right\} \tag{53}$$

Since T_b is independent of concentration, then (T_b-T_L) can be varied independent of concentration. Since each run in a set of runs has the same average composition, $\frac{1}{2}(y_{AO}+y_{AT})$, the effect of composition on λ_{mi} and $K_G a$ will be the same. For these reasons ξ will be taken independent of composition. From the argument $G/K'_G a$ is constant over the composition range and the height of the column is fixed, the value of N'_{OG} with a thermal effect should be equal to N_{OG} without the thermal effect.

$$N'_{OG}\Big|_{T_b=T_L} = N'_{OG}\Big|_{T_b\neq T_L} \tag{54}$$

The values of both functions were measured experimentally and ξ were calculated in the following manner.

$$N'_{OG}\Big|_{T_b=T_L} = \int_{y_{AO}}^{y_{AT}} \frac{dy_A}{(y_A^*-y_A)+\xi(y_A^*-y_A)} \tag{55}$$

$$N'_{OG}\Big|_{T_b=T_L} = \int_{y_{AO}}^{y_{AT}} \frac{dy_A}{(1+\xi)(y_A^*-y_A)} \tag{56}$$

$$N'_{OG}\Big|_{T_b=T_L} = \frac{1}{1+\xi} \int_{y_{AO}}^{y_{AT}} \frac{dy_A}{(y_A^*-y_A)} \tag{57}$$

$$N'_{OG}\Big|_{T_b=T_L} = \left(\frac{1}{1+\xi}\right) N_{OG}\Big|_{T_b \neq T_L} \tag{58}$$

$$\xi = \{(N_{OG}\Big|_{T_b \neq T_L}) / (N'_{OG}\Big|_{T_b=T_L})\} - 1 \tag{59}$$

The variation of ξ as a function of (T_b-T_L) is shown in Figures 23, 24 and 25. It should be noted that as the temperature approaches zero, the linear approximation breaks down. This could be explained by the fact that the adiabatic thermal term $\phi(y_A, y_{Ai})$ becomes increasingly important when $\phi'(y_A, y_{Ai}, T_b)$ becomes smaller. It is also important to note that as the average concentration approaches the intermediate concentration range, the inflection at $(T_b-T_L) = 0$ becomes smaller. This may be explained by the fact that the thermal effects due to the vapor-liquid temperature difference, $\phi(y_A, y_{Ai})$, are larger in the intermediate concentration range. The effect of the external heat source will be less compared to the effect of $\phi(y_A, y_{Ai})$ and thus show less effect when $\phi'(y_A, y_{Ai}, T_b)$ is very small.

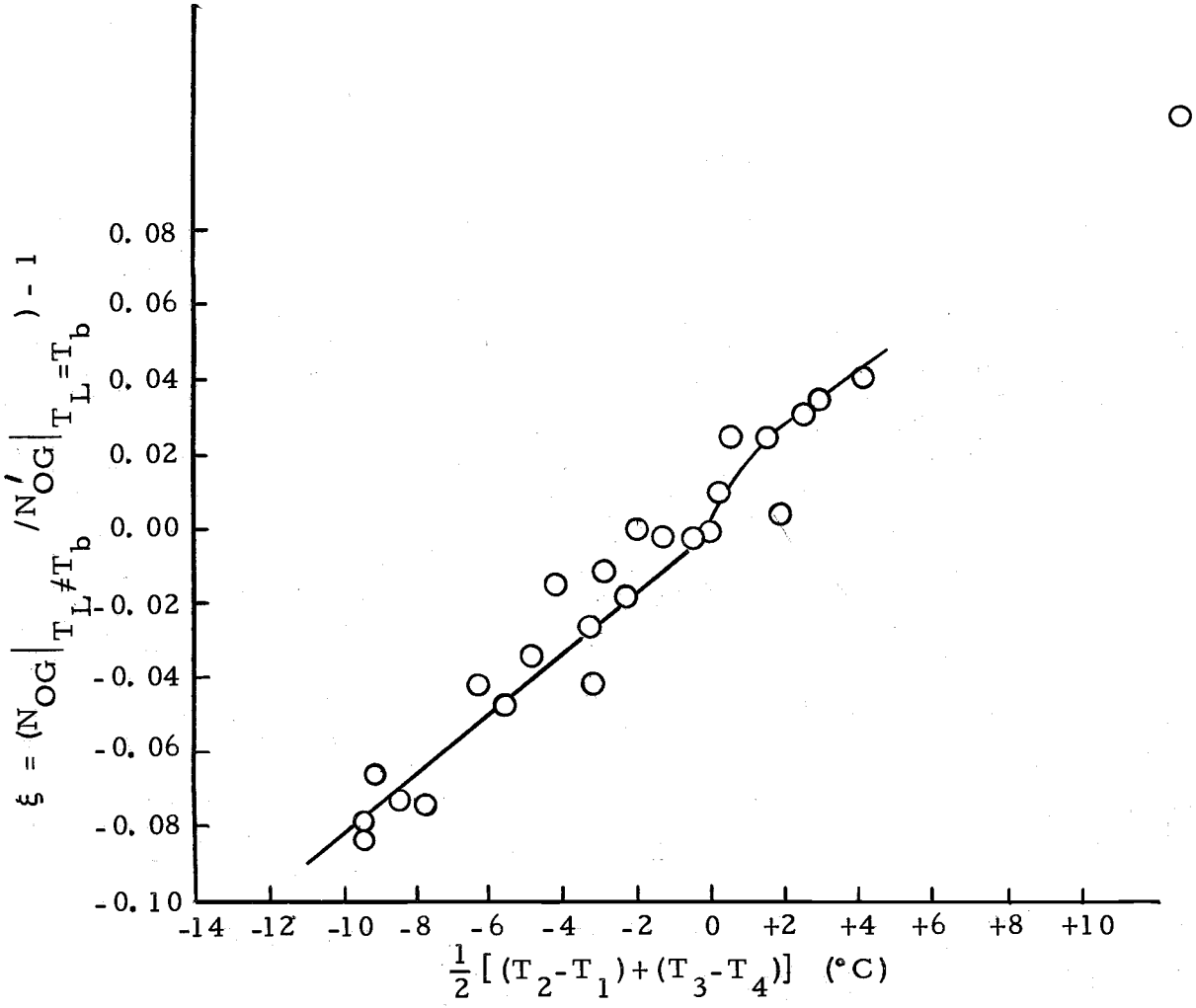

Figure 23. Non-adiabatic thermal driving force versus the average temperature difference between the heat transfer fluid and the reflux liquid.

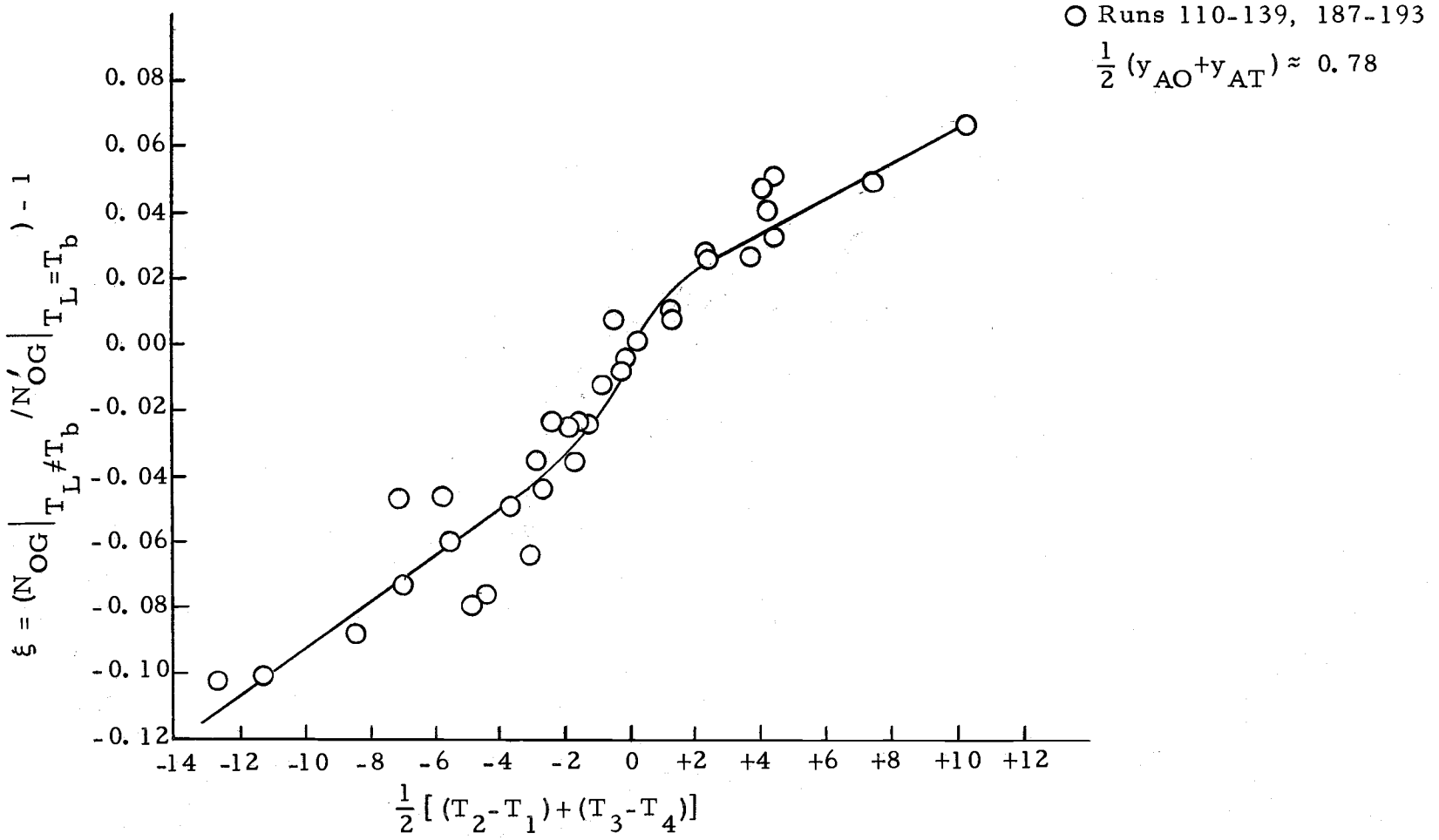

Figure 24. Non-adiabatic thermal driving force versus the average temperature difference between the heat transfer fluid and the reflux liquid.

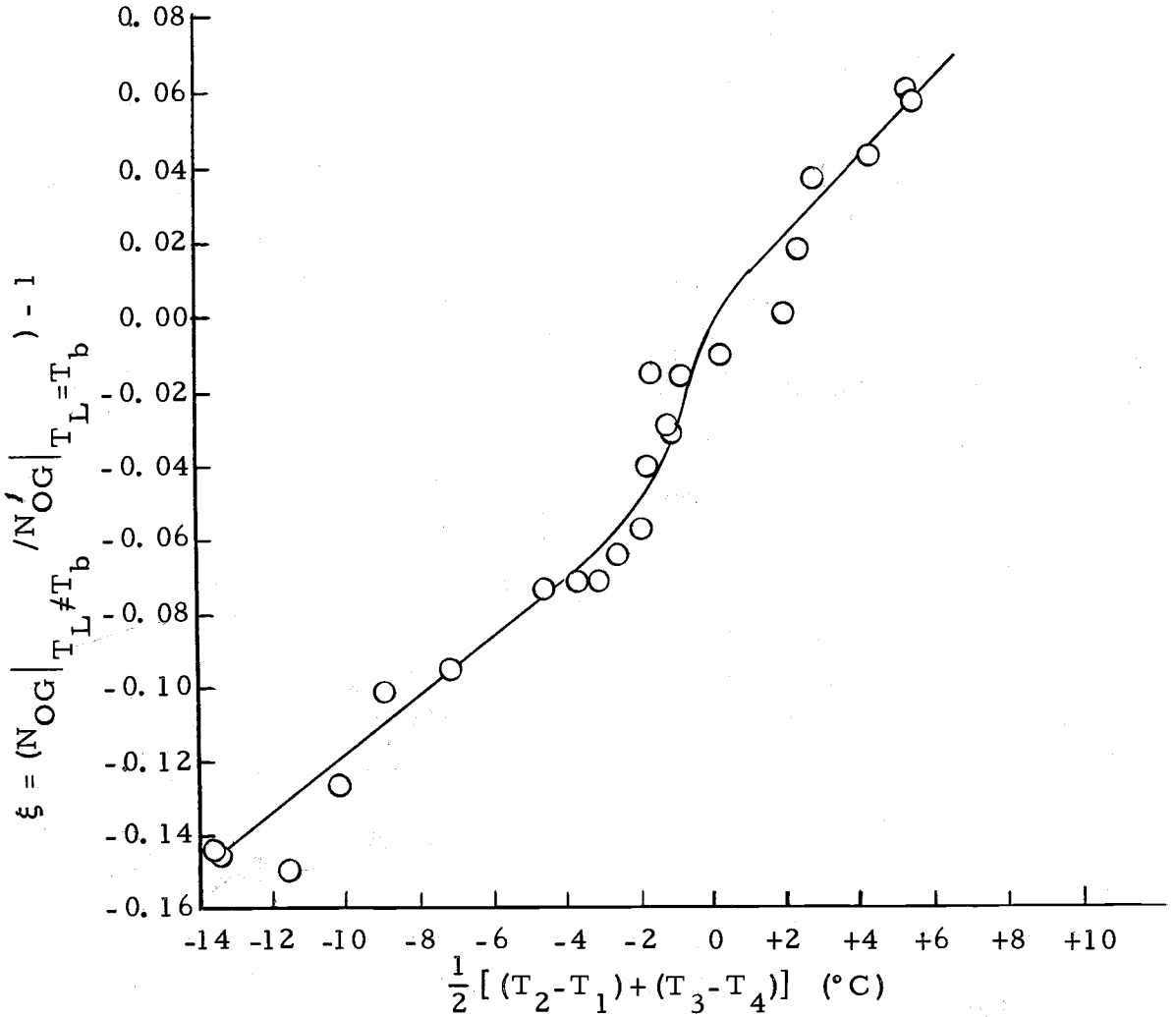

Figure 25. Non-adiabatic thermal driving force versus the average temperature difference between the heat transfer fluid and the reflux liquid.

The number of transfer units N_{OG} for both adiabatic and non-adiabatic runs are shown in Figures 26 and 27. The figures indicate that the non-adiabatic term becomes more important as the concentration approaches the pure component benzene. This would indicate the non-adiabatic term becomes increasingly important as the adiabatic term becomes smaller. Also the non-adiabatic term becomes more important relative to the concentration driving force.

A common example in industry where there is heat transferred across a physical boundary in a distillation operation would be in a plate column. Even though this is not a continuous contact operation like a wetted-wall column, the heat transferred from the vapor to the bottom of the distillation plate will have the same effect as heat added to the wetted-wall column. This effect would be to increase the separation and thus the column efficiency.

It was reasoned from the arguments presented in the discussion of the present theory that the amount of separtion, $(y_{AT}-y_{AO})$, was a function of the thermal effects. That is, the experimentally observed separation would be different than would be predicted by equations based on data where thermal effects are either non-existent or different. To be able to predict the performance of the column with a known inlet vapor composition, it would therefore be necessary to graph the number of transfer units N_{OG} versus y_{AO}. This is shown in Figure 28 over the vapor inlet composition range of 25 to 83

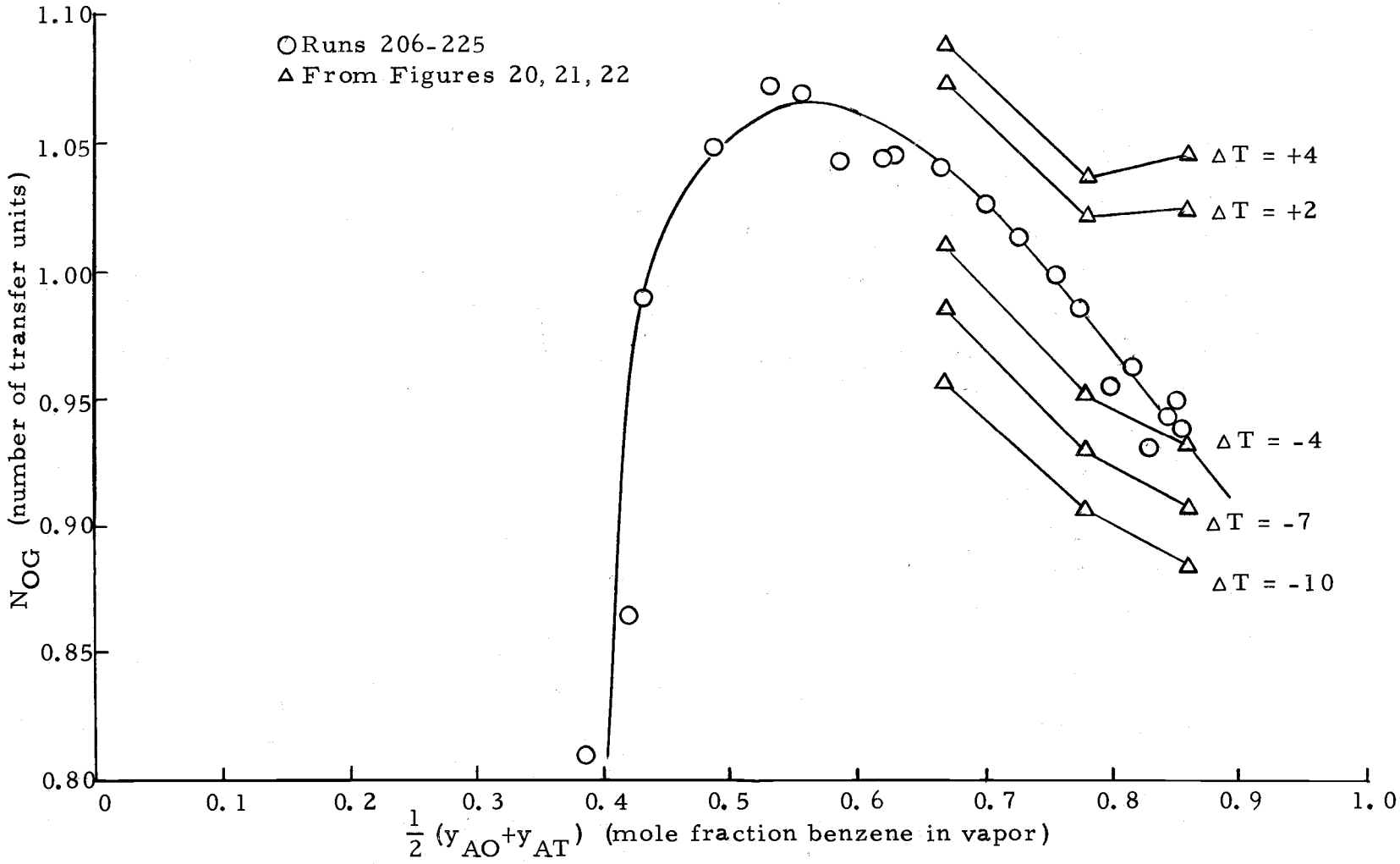

Figure 26. Comparison of N_{OG} with external heat effects and without external heat effects.

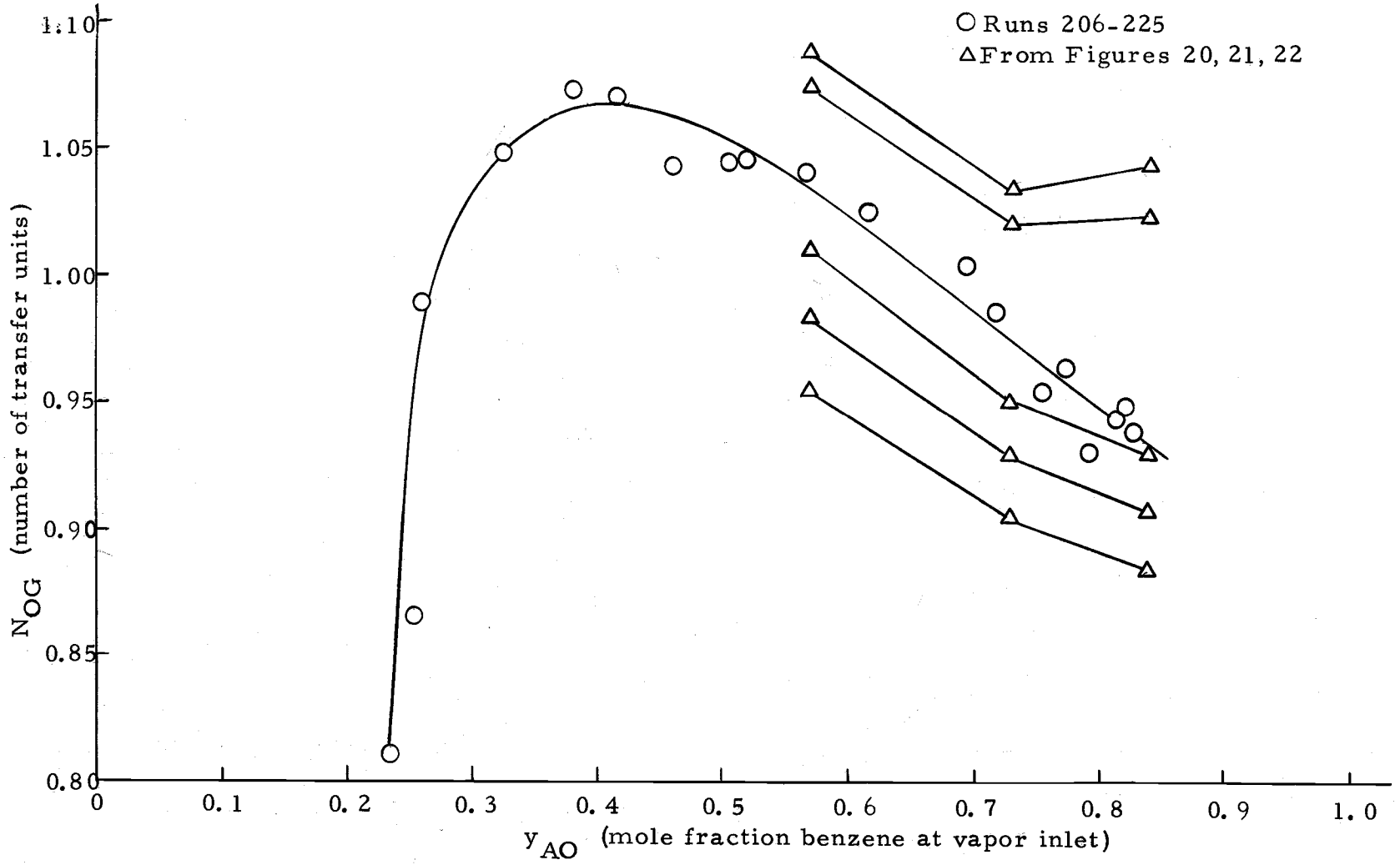

Figure 27. Comparison of N_{OG} with external heat effects and without external heat effects.

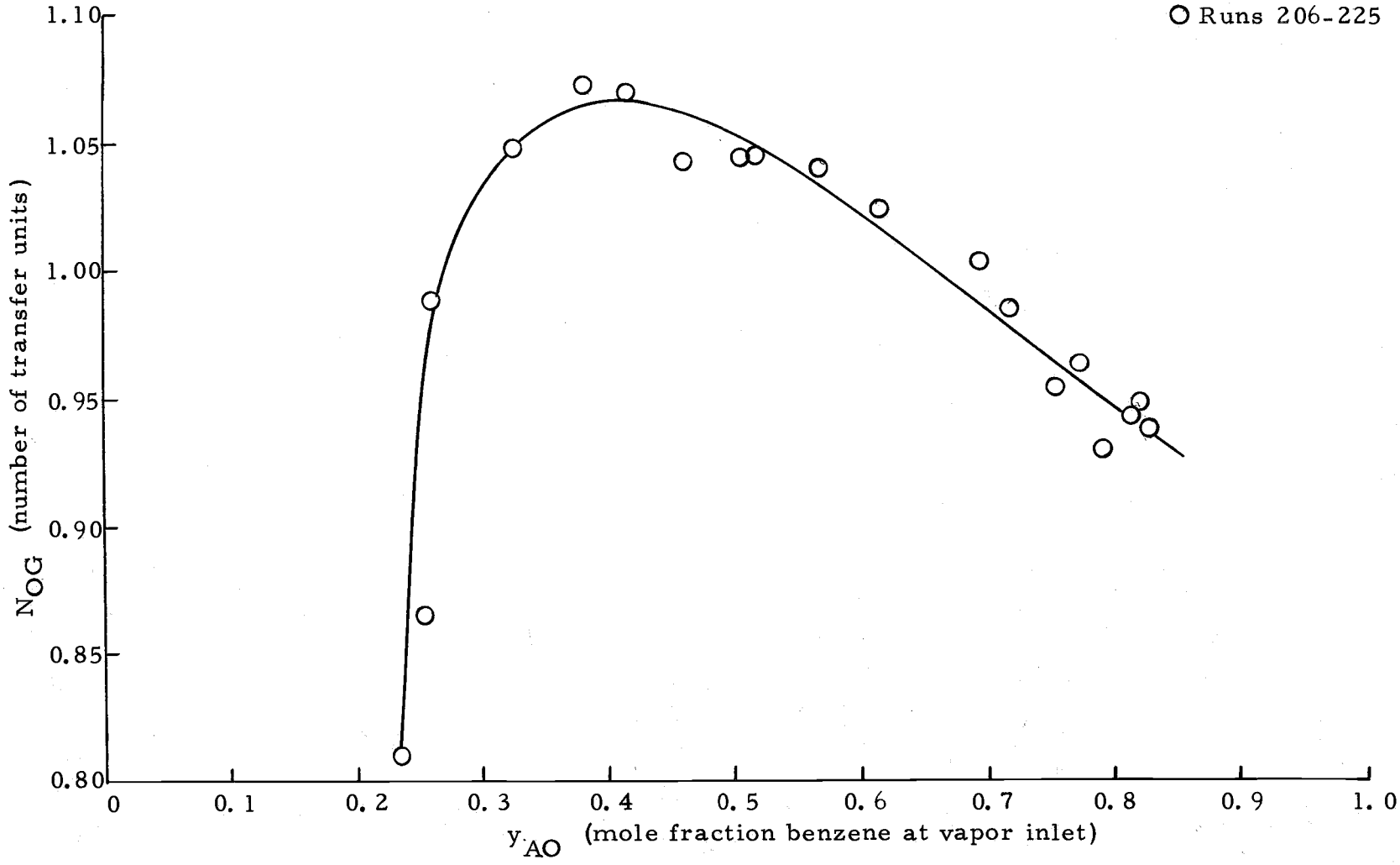

Figure 28. The number of transfer units as a function of the inlet vapor composition.

mole percent benzene. The variation of experimentally observed separation $(y_{AT}-y_{AO})$ as a function of y_{AO} is shown in Figure 29. From the previous arguments it can be seen that if the thermal effect is positive, the separation would be larger. If the thermal effect is negative, the separation would decrease. This is supported by experimental results where the non-adiabatic thermal term $\phi'(y_A, y_{Ai}, T_b)$ was varied. When $\phi'(y_A, y_{Ai}, T_b)$ was less than zero there was indeed a reduction in the separation $(y_{AT}-y_{AO})$. When $\phi'(y_A, y_{Ai}, T_b)$ was greater than zero there was an increase in the separation.

The fact that the separation $(y_{AT}-y_{AO})$ as a function of y_{AO} is linear above y_{AO} equal to 0.4 is indicative that the linear assumption necessary to obtain the average adiabatic thermal terms was reasonably good assumptions.

The surface of the liquid was rippling in all the experiments. The rippling could not be avoided because all the experiments were run with liquid Reynolds numbers between 200 and 315. It has been shown (1) that flow with Reynolds numbers greater than 25 will have ripples in the surface. Since the flow rate for smooth flow was too small for accurate measurements, it was necessary to accept these flow conditions.

The vapor was always in turbulent flow with Reynolds numbers in the range of 8,000 to 10,000. These were calculated with the velocity relative to the stationary wall of the column.

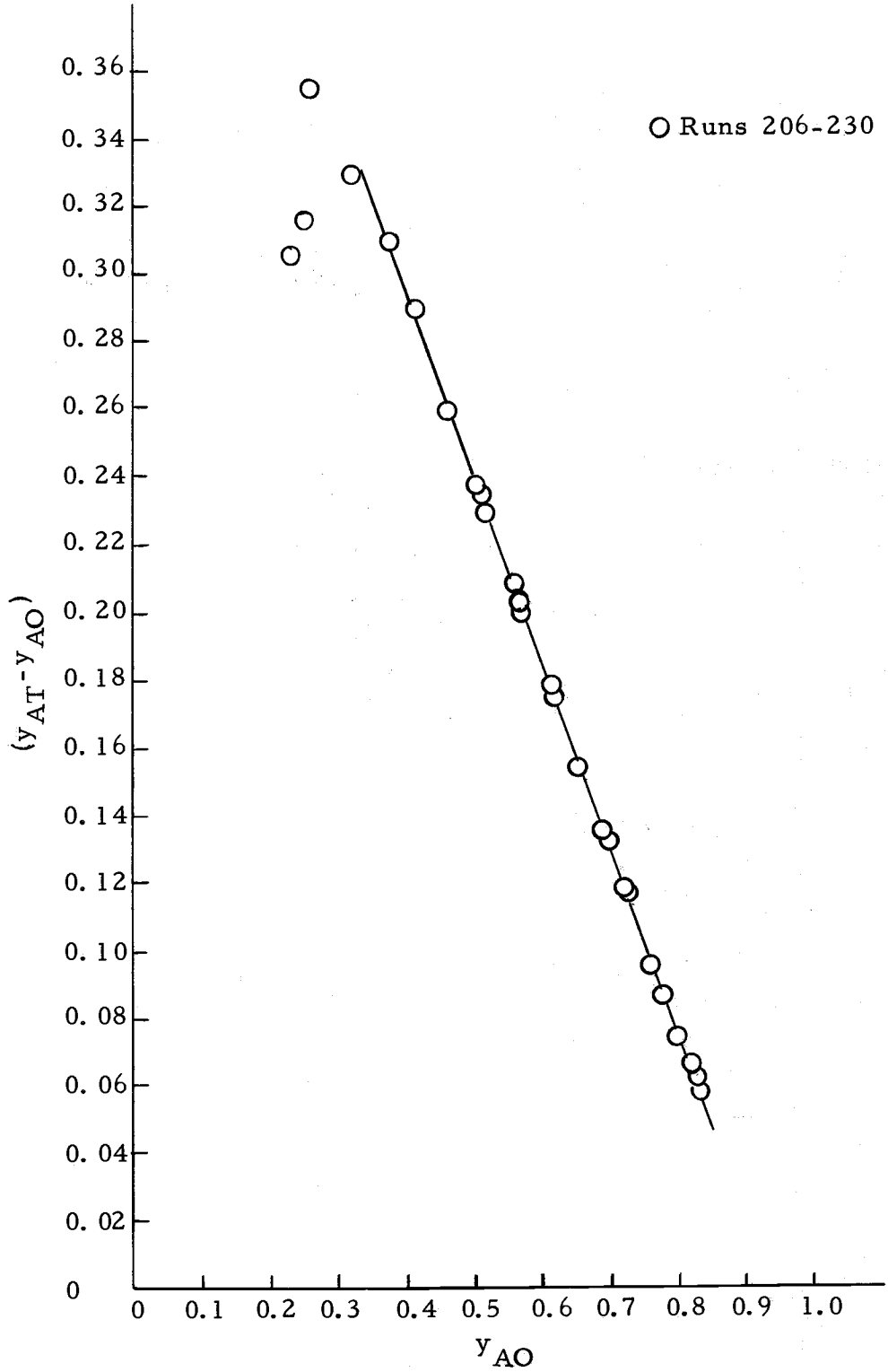

Figure 29. Separation obtained as a function of the inlet vapor composition.

CONCLUSIONS

The assumption that the amount of more volatile component vaporized was the sum of the concentration and thermal effects was made. Using this and energy balances, it was shown that the equation for the number of transfer units with thermal effects should be Equation (32).

$$N'_{OG} = \int_{y_{AO}}^{y_{AT}} \frac{dy_A}{(y_A^* - y_A) + \phi(y_A, y_{Ai}) + \phi'(y_A, y_{Ai}, T_b)} \qquad (32)$$

The modified form N'_{OG} has been shown to describe the performance of the wetted-wall distillation column under conditions where $\phi'(y_A, y_{Ai}, T_b) \gg \phi(y_A, y_{Ai})$.

RECOMMENDATIONS FOR FUTURE WORK

1. A set of systems with a large range of values for the relative volatility should be investigated and compared in terms of the various thermal contributions which are possible.
2. Systems involving two components with similar heats of vaporization should be investigated. This should yield some information on the relative importance of the sensible heat term.
3. A series of investigations could be made to show the influence of the vapor mass flow rate on the various thermal terms.

BIBLIOGRAPHY

1. Belkin, H. H. et al. Turbulent flow down vertical walls. Journal of the American Institute of Chemical Engineers 5:245-248. 1959.

2. Chapman, S. and T. G. Cowling. Mathematical theory of non-uniform gases. 2d ed. Cambridge, Cambridge University, 1951. 454 p. (Cited in: Bird, R. Byron, Warren E. Stewart and Edwin N. Lightfoot. Transport phenomena. New York, Wiley, 1960. p. 22)

3. Chari, K. S. and J. A. Storrow. Film resistances in rectification. Journal of Applied Chemistry 1:45-67. 1951.

4. Chilton, T. H. and A. P. Colburn. Distillation and absorption equipment. A convenient design and correlation method. Industrial and Engineering Chemistry 27:255-260. 1935.

5. Chilton, T. H. and A. P. Colburn. Mass transfer (absorption) coefficients. Prediction from data on heat transfer and fluid friction. Industrial and Engineering Chemistry 26:1183-1187. 1934. (Cited in: Bird, R. Byron, Warren E. Stewart, and Edwin N. Lightfoot. Transport phenomena. New York, Wiley, 1960. p. 647)

6. Colburn, A. P. Simplified calculation of diffusional processes. Industrial and Engineering Chemistry 33:459-467. 1941.

7. Colburn, A. P. The simplified calculation of diffusional processes. General consideration of two-film resistances. Transactions of the American Institute of Chemical Engineers 35:211-236. 1939.

8. Danckwerts, P. V., H. Sawistowski and W. Smith. The effects of heat transfer and interfacial tension in distillation. In: Proceedings of the International Symposium on Distillation, Brighton, England, 1960. London, Institution of Chemical Engineers, 1960. p. 7-12.

9. Dobratz, Carroll J. Heat capacities of organic vapors. Industrial and Engineering Chemistry 33:759-762. 1941. (Cited in: Perry, John H., Cecil H. Chilton and Sidney N. Kirkpatrick. Chemical Engineers' Handbook. 4th ed. New York, McGraw-Hill, 1963. p. 3-219)

10. Eucken, A. Über das warmeleitvermogen, des spezifishe Warme und der innere Reibung der Gas. Physicalische Zeitshrift 14:324-332. 1913. (Cited in: Bird, R. Byron, Warren E. Stewart and Edwin N. Lightfoot. Transport phenomena. New York, Wiley, 1960. p. 257)

11. Everitt, C. T. and H. P. Hutchison. The effect of composition on the performance of a wetted wall column. Transactions of the Institution of Chemical Engineers (London) 45:p. T9-T15. 1967.

12. Gilliland, E. R. and T. K. Sherwood. Diffusion of vapors into air streams. Industrial and Engineering Chemistry 26:516-523. 1936.

13. Hatta, Shiroji J. The theory of absorption of gases by liquids flowing in a thin layer. Journal of the Society of the Chemical Industry (Japan) 37:supplementary binding 274-277. 1934. (Cited in: Everitt, C. T. and H. P. Hutchison. The effect of composition on the performance of a wetted wall column. Transactions of the Institution of Chemical Engineers (London). Vol. 45. p. T12. 1967)

14. Hikita, H., K. Nakanishi and T. Kataoka. Liquid phase mass transfer in wetted wall columns. Chemical Engineering (Tokyo) 23:459-466. 1959. (Cited in: Hutchison, H. P. and M. A. Lusis. Distillation efficiencies of binary and ternary mixtures in a wetted wall column. Transactions of the Instituion of Chemical Engineers (London). Vol. 46. p. T160. 1968)

15. Hirschfelder, Joseph O., R. Byron Bird and Ellen L. Spotz. The transport properties of gases and gaseious mixtures. Chemical Reviews 44:205-231. 1949. (Cited in: Bird, R. Byron, Warren E. Stewart and Edwin N. Lightfoot. Transport phenomena. New York, Wiley, 1960. p. 246)

16. Hochgesand, Gerhard. Einfluss von Kondensation und Verdampfung auf den Stoffaustaush bei der Rectification. Chemie-Ingenieur-Technik 34:178-82. 1962.

17. Hutchison, H. P. and M. A. Lusis. Distillation efficiencies of binary and ternary mixtures in a wetted wall column. Transactions of the Institution of Chemical Engineers (London) 46:T158-T166. 1968.

18. Kendall, James and Kenneth Potter Monroe. The viscosity of liquids, II. The viscosity-composition curve for ideal mixtures. Journal of the American Chemical Society 39:1787-1802. 1917. (Cited in: Perry, John H., Cecil H. Chilton and Sidney N. Kirkpatrick (eds.). Chemical Engineers' Handbook. 4th ed. New York, McGraw-Hill, 1963. p. 3-229)

19. Kirschbaum, E. Destiller-und Rektifiziertechnik. 1st ed. Berlin, Springer Verlag, 1940. p. 236-238. (Cited in: Danckwerts, P. V., H. Sawistowski and W. Smith. The effects of heat transfer and interfacial tension in distillation. In: Proceedings of the International Symposium on Distillation, Brighton, England, 1960. London, Institution of Chemical Engineers, 1960. p. 7)

20. Kreith, Frank. Principles of heat transfer 2d ed. Scranton, International Book, 1965. 620 p.

21. LeBas, G. The molecular volumes of liquid chemical compounds from the point of view of Kopp.. London, Longmans, 1915. (Cited in: Perry, John H., Cecil H. Chilton and Sidney N. Kirkpatrick (eds.). Chemical Engineers' Handbook. 4th ed. New York, McGraw-Hill, 1963. p. 14-20)

22. Liang, S. Y. and W. Smith. The effect of heat transfer between the phases on the performance of countercurrent distillation columns. Chemical Engineering Science 17:11-21. 1959.

23. Mrazek, Robert V. and H. C. VanNess. Heats of mixing: Alcohol-aromatic binary systems at 25°, 35° and 45°C. Journal of the American Institute of Chemical Engineers 7:190-195. 1961.

24. Nusselt, Wilhelm. Die Oberflachenkondensation des Wasserdampfes. Zeitschrift des Vereins Deutscher Ingenieure 60:541-546. 1916. (Cited in: Belkin, H. H. et al. Turbulent flow down vertical walls. Journal of the American Institute of Chemical Engineers 5:p. 245. 1959)

25. Perry, John H., Cecil H. Chilton and Sidney N. Kirkpatrick (eds.). Chemical Engineers' Handbook. 4th ed. New York, McGraw-Hill, 1963. 26-45 p.

26. Pratt, H. R. C. The performance of packed columns with particular reference to wetting. Transactions of the Institution of Chemical Engineers (London) 29:195-214. 1951. (Cited in: Sawistowski, Henryk and William Smith. Performance of packed distillation columns. Industrial and Engineering Chemistry. Vol. 51. p. 916. 1959)

27. Quershi, A. K. and W. Smith. The distillation of binary and ternary mixtures. Journal of the Institute of Petroleum 44:127-146. 1958.

28. Reynolds, A. E. and T. DeVries. The heat capacity of organic vapors. Journal of the American Chemical Society 72:5443-5445. 1950.

29. Rossini, Fredrick D. et al. Selected values of physical and thermodynamic properties of hydrocarbons and related compounds. American Petroleum Institute Research Project 44, Carnegie Institute of Technology, Pittsburgh, 1953. (Cited in: Himmelblau, David M. Basic principles and calculations in chemical engineering. Englewood Cliffs, New Jersey, Prentice-Hall, 1962. p. 417)

30. Sawistowski, Henryk and William Smith. Performance of packed distillation columns. Industrial and Engineering Chemistry 51: 915-918. 1959.

31. Steudel, Wilhelm and Ernst Hofman. Verzeichniss wurttembergischer Kleinschmetterlinge. Württemberg, Jahreshefte 38:143-262. 1882. (Cited in: Hodgman, Charles D., et al. Handbook of chemistry and physics. 43d ed. Cleveland, Chemical Rubber Company, 1961. p. 2219)

32. Van Ness, H. C. Classical thermodynamics of nonelectrolytic solutions. New York, Pergamon, 1964. 166 p.

33. Whitman, Walter G. A preliminary experimental confirmation of the two-film theory of gas absorption. Chemical and Metallurgical Engineering 29:146-148. 1923.

34. Wilke, C. R. and Pin Chang. Correlation of diffusion coefficients in dilute solutions. Journal of the Institute of Chemical Engineers 1:264-270. 1955. (Cited in: Perry, John H., Cecil H. Chilton and Sidney N. Kirkpatrick. Chemical Engineers' Handbook. 4th ed. New York, McGraw-Hill, 1963. p. 14-21)

35. Yerazunis, S., J. D. Plowright and F. M. Smola. Vapor-liquid equilibrium determination by a new apparatus. Journal of the American Institute of Chemical Engineers 10:660-665. 1964.

36. Zuiderweg, F. J. and A. Harmens. The influence of surface phenomena on the performance of distillation columns. Chemical Engineering Science 9:89-103. 1958.

APPENDICES

APPENDIX A

Nomenclature

Symbol	Definition	Units
a	surface area per volume	1/cm
A	subscript, more volatile component	dimensionless
B	subscript, less volatile component	dimensionless
C_{PG}	heat capacity of gas phase	cal/gmole°C
C_{PL}	heat capacity of liquid phase	cal/gmole°C
D_{AB}	mass diffusivity, A through B	cm^2/sec
D_G	mass diffusivity in gas phase	cm^2/sec
D_L	mass diffusivity in liquid phase	cm^2/sec
D_t	tube diameter	cm
G	vapor molar velocity	$gmoles/cm^2sec$
g	acceleration of gravity	cm/sec^2
h_A	specific enthalpy of A in liquid	cal/gmole
h_B	specific enthalpy of B in liquid	cal/gmole
h_b	heat transfer coefficient between heat transfer fluid and reflux liquid	$cal/cm^2sec°K$
H_G	specific enthalpy of vapor mixture	cal/gmole
H_L	specific enthalpy of liquid mixture	cal/gmole

Symbol	Definition	Units
ΔH_m	molar heat of mixing	cal/gmole
H_{OG}	height of transfer unit, overall gas phase	cm
H'_{OG}	height of transfer unit, overall gas phase including thermal effects	cm
H_{TG}	height of transfer unit, gas phase	cm
H_{TL}	height of transfer unit, liquid phase	cm
h_V	heat transfer coefficient between vapor and liquid phases	cal/cm^{2}sec°K
i	subscript, interfacial conditions	dimensionless
k	thermal conductivity	cal-cm/cm^{2}sec°K
k_G	gas phase individual mass transfer coefficient	gmole/cm^{2}sec
K_G	gas phase overall mass transfer coefficient	gmole/cm^{2}sec
K'_G	gas phase overall mass transfer coefficients including thermal effects	gmole/cm^{2}sec
k_L	liquid phase individual mass transfer coefficient	gmole/cm^{2}sec
L	liquid molar velocity	gmole/cm^{2}sec
m	slope of vapor-liquid equilibrium	dimensionless
M	average molecular weight	dimensionless
M_B	molecular weight of B	dimensionless
n	Quershi and Smith, exponent	dimensionless

Symbol	Definition	Units
$\vec{N}_A$	mass flux of A, r-component	gmoles/cm^2sec
$\vec{N}'_A$	mass flux of A including thermal effects, r-component	gmoles/cm^2sec
$\vec{N}_B$	mass flux of B, r-component	gmole/cm^2sec
$\vec{N}'_B$	mass flux of B including thermal effects, r-component	gmole/cm^2sec
N_{OG}	number of transfer units, overall gas phase	dimensionless
N'_{OG}	number of transfer units, overall gas phase including thermal effects	dimensionless
P	pressure	atmospheres
Pr_G	Prandtl number, gas, $Cp\mu/k$	dimensionless
Pr_L	Prandtl number, liquid, $Cp\mu/k$	dimensionless
R	gas constant	atm cm^3/gmole°K
r	radius of tube	cm
Re_G	Reynolds number, gas, $Dv\rho/\mu$	dimensionless
Re_L	Reynolds number, liquid, $Dv\rho/\mu$	dimensionless
Sc_G	Schmidt number, gas, μ/DM	dimensionless
Sc_L	Schmidt number, liquid, μ/DM	dimensionless
T	temperature	°C
T_b	temperature of heat transfer fluid	°C
T_G	temperature, average, gas phase	°C

Symbol	Definition	Units
T_i	temperature at vapor-liquid interface	°C
T_L	temperature, average, liquid phase	°C
T_{ref}	temperature, reference, liquid enthalpy	°C
V_O	molal volume of solute at normal boiling point	$cm^3/gmole$
X	association parameter	dimensionless
x_A	mole fraction A in liquid	dimensionless
x_i	mole fraction at vapor-liquid interface	dimensionless
x_L	mole fraction, average, liquid	dimensionless
y_A	mole fraction A in gas phase	dimensionless
y_A^*	mole fraction A in equilibrium with y_A	dimensionless
y_{Ai}	mole fraction A at interface, vapor	dimensionless
y_{AO}	mole fraction A in vapor at vapor inlet	dimensionless
y_{AT}	mole fraction A in vapor at vapor outlet	dimensionless
z	height in tube	cm
δ	liquid film thickness	cm
θ	molar flux due to all thermal effects	$moles/cm^2 sec$

Symbol	Definition	Units
λ_{Ai}	molar heat of vaporization of A at vapor-liquid interface conditions	cal/gmole
λ_{Bi}	molar heat of vaporization of B at vapor-liquid interface conditions	cal/gmole
λ_{mi}	average molar heat of vaporization of mixture at interfacial conditions	cal/gmole
μ_A	viscosity of A	gm/cm sec
μ_B	viscosity of B	gm/cm sec
μ_L	viscosity of liquid	gm/cm sec
μ_m	viscosity of mixture, liquid	gm/cm sec
ξ	thermal coefficient, to over-all gas driving force	dimensionless
π	mathematical constant, 3.14	dimensionless
ρ	mass density	gm/cm^3
σ_{AB}	collision diameter	cm
$\phi(y_A, y_{Ai})$	adiabatic thermal driving force	dimensionless
$\phi'(y_A, y_{Ai}, T_b)$	non-adiabatic thermal driving force	dimensionless
Ω_D	collision integral for diffusion	dimensionless
Ω_μ	collision integral for viscosity	dimensionless

APPENDIX B

Vapor-Liquid Equilibrium Data by Yerazunis, Plowright, and Smola (35)

Isobaric conditions at 760 mm. Hg.

Temperature (°C)	Mole fraction benzene in liquid phase	Mole fraction benzene in vapor phase
	1.0000	1.0000
80.23	0.9805	0.9822
80.35	0.9535	0.9617
80.49	0.9265	0.9462
80.64	0.9075	0.9389
80.80	0.8854	0.9283
81.32	0.8255	0.9085
82.37	0.7279	0.8839
84.18	0.5965	0.8501
87.37	0.4329	0.7955
87.89	0.4230	0.7867
92.45	0.3030	0.7129
93.87	0.2683	0.6823
97.67	0.2031	0.6076
97.82	0.1994	0.6026
109.04	0.0647	0.2968
114.57	0.0215	0.1152
115.74	0.0117	0.0693
116.56	0.0062	0.0395

Run No.	TC1 °C	TC2 °C	TC3 °C	TC4 °C	TC5 °C	TC6 °C	TC7 °C	TC8 °C	Rotameter 1 gm/min	Rotameter 2 gm/min	Mole fract. at Sample Point A (y_{AT})	Mole fract. at Sample Point B (y_{AO})
117	82.1	84.7	84.5	79.7	90.2	84.0	72.9	71.0	----	122.5	.8398	.7272
118	82.0	80.4	80.7	80.0	90.55	84.4	72.5	70.8	----	122.5	.8354	.7214
119	82.0	74.9	75.4	80.0	90.0	84.0	70.3	70.7	114.6	122.5	.8320	.7228
120	82.0	73.5	74.1	80.0	90.6	84.4	70.5	71.0	106.0	117.8	.8296	.7180
121	81.8	72.1	73.0	80.3	90.7	84.4	70.8	71.0	106.0	117.8	.8288	.7214
122	81.9	69.8	70.5	81.1	90.4	84.65	70.5	71.1	101.0	122.5	.8280	.7240
123	82.25	68.3	69.1	80.55	91.0	84.8	69.4	71.3	91.5	117.8	.8242	.7182
124	81.8	73.7	74.3	80.25	90.1	84.25	70.5	70.1	108.4	117.8	.8306	.7242
125	81.9	75.3	75.8	80.4	90.65	84.4	70.8	70.9	115.0	120.2	.8280	.7168
126	82.0	77.0	77.45	79.7	90.6	84.0	71.3	71.3	----	120.2	.8324	.7234
127	82.4	85.1	85.0	79.7	----	----	----	----	----	123.9	.8310	.7050
128	82.2	85.45	85.35	80.2	91.0	84.2	72.8	71.5	----	122.5	.8374	.7200
129	82.1	81.5	81.8	80.7	90.8	84.0	72.0	70.9	----	121.5	.8340	.7190
130	81.8	83.8	83.55	80.7	89.1	83.5	72.7	70.1	----	122.5	.8450	.7394
131	82.0	82.5	82.7	80.7	89.9	83.8	71.8	71.0	----	120.2	.8424	.7352
132	82.0	81.2	81.5	80.9	90.1	84.0	72.7	70.4	----	120.2	.8382	.7290
133	82.2	80.4	80.8	80.8	90.6	84.5	73.1	70.4	----	119.2	.8370	.7278
134	82.1	79.4	79.9	80.4	90.45	84.3	73.0	70.4	----	119.2	.8352	.7256
135	82.2	91.3	91.1	79.9	91.65	84.3	72.2	70.2	----	115.4	.8338	.7082
136	82.5	88.5	88.9	80.1	91.9	84.4	72.4	71.3	----	112.8	.8272	.6966
137	82.0	83.75	84.2	80.9	88.9	----	----	----	----	117.8	.8546	.7628
138	82.3	86.0	86.5	81.4	90.5	84.4	73.2	70.5	----	115.4	.8398	.7236
139	82.1	85.5	85.9	80.5	90.7	84.3	72.7	71.5	----	116.7	.8360	.7182
140	82.0	85.4	85.7	80.1	91.0	83.4	72.3	75.3	----	111.7	.8330	.7064
160	86.5	75.9	76.5	81.5	99.7	89.5	70.0	78.5	112.5	120.2	.7598	.5740
161	85.25	84.85	84.5	80.3	98.8	88.2	70.4	77.6	140.5	117.7	.7705	.5740
162	85.1	81.9	81.9	79.8	98.5	88.3	70.4	77.2	130.2	117.7	.7740	.5834
163	84.7	86.2	86.2	79.5	99.2	88.1	70.0	77.3	143.2	117.7	.7740	.5714
164	84.4	85.2	85.0	79.9	98.5	88.0	70.4	76.5	141.9	117.7	.7776	.5810
165	85.0	85.1	84.8	80.0	99.1	88.5	70.7	77.0	139.6	117.7	.7735	.5729

(continued)

Run No.	TC1 °C	TC2 °C	TC3 °C	TC4 °C	TC5 °C	TC6 °C	TC7 °C	TC8 °C	Rotameter 1 gm/min	Rotameter 2 gm/min	Mole fract. at Sample Point A (y_{AT})	Mole fract. at Sample Point B (y_{AO})
166	85.7	84.3	84.3	80.0	99.6	88.6	70.9	78.0	138.1	117.7	.7684	.5632
167	85.55	83.2	83.3	80.6	99.5	88.7	71.0	77.2	132.9	117.7	.7649	.5599
168	85.4	82.9	82.9	79.5	99.3	88.7	71.0	77.8	135.5	117.7	.7703	.5677
169	84.7	80.3	80.4	80.0	99.4	89.0	70.4	77.2	126.2	117.7	.7660	.5654
170	84.9	79.9	80.1	80.5	99.7	89.5	70.8	77.6	121.0	117.7	.7668	.5702
171	84.7	78.1	78.3	80.1	98.5	88.5	69.9	78.0	119.8	117.7	.7698	.5778
172	84.7	77.75	78.1	81.0	99.0	89.2	70.6	77.7	119.8	117.7	.7660	.5730
173	83.6	80.6	80.8	80.4	97.8	88.0	70.5	76.2	128.8	117.7	.7690	.5700
174	84.7	76.5	76.8	81.3	98.6	89.1	69.8	76.7	114.8	117.7	.7655	.5760
175	85.6	74.1	74.55	81.35	98.5	89.2	70.0	76.0	105.5	117.7	.7604	.5724
176	84.8	74.6	75.1	81.7	98.1	89.7	70.7	78.2	110.2	120.2	.7594	.5724
177	84.9	73.7	74.1	81.7	98.7	89.8	70.5	78.3	110.2	120.2	.7573	.5695
178	84.7	73.5	74.0	81.6	98.7	90.0	70.55	78.55	111.3	121.6	.7536	.5636
179	84.8	79.6	79.7	80.9	99.1	89.3	71.0	78.5	126.2	121.6	.7646	.5702
180	85.0	77.2	77.5	80.9	99.7	90.0	70.6	78.5	119.8	123.0	.7580	.5618
181	85.3	79.55	79.8	80.5	99.3	89.3	70.7	78.5	128.8	124.2	.7646	.5700
182	85.7	80.7	89.9	80.5	99.6	89.5	70.7	78.5	131.5	124.2	.7646	.5678
183	85.4	----	----	81.3	99.1	89.4	70.7	78.0	134.3	124.2	.7666	.5695
184	85.6	----	----	81.0	99.55	89.2	69.9	77.9	128.8	117.7	.7646	.5659
185	81.9	75.7	76.0	80.3	90.0	84.4	67.2	74.5	108.6	120.1	.8340	.7325
186	82.2	78.2	78.2	80.4	89.1	83.7	68.5	----	115.4	120.1	.8382	.7386
187	81.7	79.6	79.7	80.2	89.4	83.55	68.45	75.8	119.2	117.6	.8413	.7385
188	82.1	81.9	82.1	79.9	90.4	84.0	68.85	75.4	126.3	120.7	.8424	.7360
189	81.9	83.6	83.15	80.2	90.3	83.8	69.8	76.0	142.7	118.4	.8370	.7212
190	82.2	81.3	81.2	80.9	90.55	84.2	69.9	76.3	125.2	118.4	.8338	.7207
191	82.4	79.15	79.15	80.7	91.1	84.6	68.4	76.5	129.0	121.4	.8270	.7086
192	81.8	79.7	79.6	81.0	89.7	84.0	68.3	75.9	119.2	117.6	.8368	.7308
193	82.1	77.7	77.9	79.7	90.75	84.65	67.4	76.2	113.6	118.9	.8278	.7164
198	80.7	76.75	76.85	80.2	83.2	81.2	64.9	63.3	103.7	113.7	.8880	.8354
199	80.3	78.7	78.9	80.9	83.6	81.45	67.3	73.1	107.2	114.0	.8884	.8340

(continued)

Run No.	TC1 °C	TC2 °C	TC3 °C	TC4 °C	TC5 °C	TC6 °C	TC7 °C	TC8 °C	Rotameter 1 gm/min	Rotameter 2 gm/min	Mole fract. at Sample Point A (y_{AT})	Mole fract. at Sample Point B (y_{AO})
200	80.6	80.7	80.7	80.5	83.45	81.35	66.4	72.9	117.0	113.3	.8900	.8346
201	80.3	82.8	82.8	80.7	83.4	81.4	68.45	73.1	123.3	114.0	.8904	.8332
202	80.9	83.1	83.2	80.6	83.2	81.35	67.5	73.2	122.2	113.3	.8924	.8384
203	80.1	84.3	84.3	80.0	82.9	80.7	68.9	73.9	127.2	111.8	.8935	.8375
204	80.0	86.2	85.9	79.5	82.8	80.5	68.1	72.8	134.8	111.8	.8918	.8346
205	80.7	----	----	81.8	83.65	81.6	64.2	72.9	107.2	111.8	.8900	.8356
206	97.3	----	----	83.9	110.2	100.0	74.1	91.0	117.1	118.9	.5364	.2356
207	96.7	----	----	83.4	109.8	98.4	73.8	90.0	118.8	119.4	.5650	.2540
208	97.3	----	----	83.0	110.0	97.0	73.0	90.0	118.2	118.9	.6050	.2601
209	92.5	----	----	81.2	108.0	93.8	71.55	86.5	121.2	119.6	.6494	.3244
210	89.2	----	----	82.1	105.0	92.3	71.4	82.8	119.8	114.8	.700	.4152
211	90.3	----	----	82.5	106.0	93.0	70.0	84.2	125.7	117.8	.6850	.3800
212	88.0	----	----	81.4	102.9	90.9	71.7	81.0	126.0	119.1	.7152	.4595
213	86.2	----	----	82.2	100.8	90.0	72.0	81.5	128.7	118.5	.7380	.5040
214	85.6	----	----	82.1	100.5	89.1	71.0	79.4	119.0	112.6	.7448	.5183
215	84.7	----	----	81.9	98.4	88.15	71.3	78.7	119.0	115.4	.7666	.5664
216	84.25	----	----	81.9	96.45	86.9	70.4	78.2	120.2	115.4	.7868	.6145
217	82.9	----	----	81.1	94.4	85.7	69.65	76.7	118.2	116.0	.8028	.6510
218	82.3	----	----	81.8	94.8	84.7	69.3	75.8	118.7	116.8	.8214	.6915
219	82.1	----	----	80.7	90.8	84.4	69.2	75.35	115.9	116.0	.8324	.7160
220	81.4	----	----	80.7	88.0	83.1	68.5	74.5	120.8	120.7	.8476	.7537
221	81.7	----	----	81.0	87.2	82.9	68.4	74.5	115.0	119.2	.8582	.7740
222	81.2	----	----	80.5	86.2	81.3	68.0	74.0	115.0	120.1	.8658	.7926
223	80.9	----	----	80.8	84.7	81.6	67.6	73.8	114.7	120.8	.8771	.8129
224	80.8	----	----	80.6	84.1	81.6	67.7	73.7	112.8	119.8	.8820	.8212
225	80.9	----	----	80.7	84.05	81.45	67.55	73.7	112.8	119.8	.8842	.8270
226	85.7	----	----	81.4	101.7	89.9	70.1	79.8	116.8	110.0	.7420	.5102
227	84.5	----	----	81.35	98.6	88.2	69.7	78.1	117.2	110.2	.7644	.5586
228	84.5	----	----	81.7	96.9	87.2	69.7	77.5	115.3	110.7	.7890	.6130
229	82.4	----	----	81.2	92.3	84.5	68.2	75.2	111.0	111.3	.8198	.6871